ABSTRACT

Accelerator design usually requires that the betatron tune is kept away from key values which would allow for the growth of transverse particle oscillations due to resonant conditions driven by lattice imperfections (the consequence of which being that particles with increasing transverse amplitude will eventually collide with the accelerator wall). The non-scaling fixed field alternating gradient (NS-FFAG) accelerator allows the betatron tune to vary with particle momentum and in doing so to cross conventionally forbidden values.

This dissertation project looks at the approximation of the proof of principle linear NS-FFAG accelerator EMMA (Electron Machine with Many Applications) to a constant gradient accelerator, with the aim of simulating the transverse amplitude growth that occurs as a result of crossing integer betatron tune values and transverse misalignment in quadrupole positions.

The influence of the magnitude of the quadrupole alignment errors and the rate of acceleration are studied, and the results from this approximate model are compared to those obtained using a 'full physics' model[1].

RESULTS

- The constant gradient approximated model was found to be able to demonstrate the same features of integer tune crossing as a 'full physics' model.
- The amplitude growth as a function of acceleration rate was found to have a gradient of $(38 \pm 1\,)m^{-1/2}$ (3% error).
- The success of a linear NS-FFAG in being able to accelerate particles to extraction energy, was found to be dependent upon the rate of acceleration.

[1] Machida, S. (2008) *Resonance Crossing and Dynamic Aperture in Non-scaling Fixed Field Alternating Gradient Accelerators*

'full physics' is here defined as model which does not make the approximation of alternating gradient focusing to being constant gradient.

CONTENTS

SECTION I – INTRODUCTION

The Non-Scaling Fixed Field Alternating Gradient (NS-FFAG) accelerator is a novel accelerator design upon which the British Accelerator and Radiation Oncology Consortium (BASROC) intend to base a proton therapy facility. The NS-FFAG has the potential to give both economical and practical advantages over cyclotron and synchrotron alternatives when applied to the field of oncology.

RADIATION THERAPY FOR TREATING CANCER

The first page of the British Accelerator Science and Radiation Oncology Consortiums (BASROC) website claims that one third of all UK residents will, at some time, suffer from cancer, and that it can be expected that the treatment for half of these people will involve radiation therapy[2].

Radiation therapy (or radiotherapy) utilises ionizing radiation for the aim of destroying cancerous cells. Tumours made up of cancerous cells are found in the midst of healthy, functioning tissue, and so there is the constraint upon the application of radiotherapy that healthy cells must be preserved to the greatest possible degree. In fact, an effective treatment is often a compromise between the probability of eradicating the cancer and the probability of complications due to normal tissue damage[3].

Teletherapy (meaning distant therapy) involves a beam of particles emitted from a source being directed at a tumour. The dose (which may be defined as the energy deposited per unit mass JKg^{-1}) given to a specific volume within patient is determined by the way in which the beams particles deposit energy along the beam path[4]. The characteristics of this deposition of energy are specific to the type of particle used (see graph 1).

[2] BASROC. (2006) *British Accelerator Science and Radiation Oncology Consortium.* Available at http://www.basroc.org.uk/index.htm

[3] Fenwick, J. (2010) *Biological Modelling.* PHYS384:Radiation Therapy Applications Notes.

[4] Wu Chao, A. & Tigner, M. (1999) *Handbook of accelerator physics and engineering.*

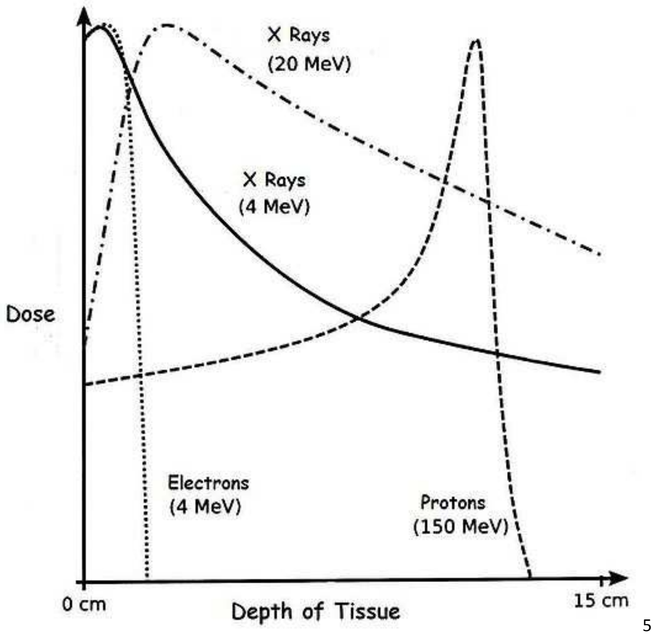

Graph 1: Depth-dose curves for photons, electrons and protons.

Currently electron and photon based treatments dominate the field of radiotherapy; however the use of other particles may offer distinct advantages. Below is a brief summary of the features seen for the particles detailed in the depth dose curves of graph 1:

Electrons:

Electrons for clinical use may be accelerated, by linear accelerator, from low energies to energies suited to therapeutic application (typically within the range 4MeV to 20MeV). An electron beam will give a relatively uniform dose with depth until rapidly falling off (at approximately 2cm for the 4MeV beam), giving a close to ideal dose distribution for superficial tumours, with little damage caused beyond the depth of the tumour.

An electron loses energy at a greater rate towards the end of its range, however the low electron mass means that it is readily scattered through large angles and that the tissue depth is not synonymous with the electron path length. It is for this reason that the uniform dose with depth is realised.

[5] Paul, H. (2009) *Depth Dose Curves*. Available at http://en.wikipedia.org/wiki/File:Depth_Dose_Curves.jpg

Photons:

Therapeutic photon production may be based on the same linear accelerators used in generating therapeutic electrons, the difference being that the accelerated electrons are incident upon a high atomic number metal target (usually tungsten).

Photons are classified by the potential through which the electrons used to generate them are accelerated, e.g. 6MV photon spectrum created through Bremstrahlung emissions as 6MeV electrons are incident upon a tungsten target. The offset in the maximum of the depth-dose curve from a 0cm depth (see graph 1) is dependent upon the energy of the beam (with high energy beams exhibiting greater offsets). This is a useful feature as it means limited dosage at the surface (skin, hence reducing patient discomfort), and a potentially higher dosage at the tumour depth. Beyond the maximum, the dose falls off exponentially with depth.

Taking a small tumour, starting at a depth of 1.5cm and extending through to 2.5cm, as an example, it can be seen from graph 1 that treatment with a 6MV photon beam would result in a significant dose being delivered before and after the tumour.

Protons:

The rate at which a proton deposits energy in tissue increases rapidly shortly before it comes to rest, the relatively large proton mass (when compared to that of an electron) leads to little scattering within tissue, and so tissue depth and proton path length are similar. A beam of monoenergetic protons incident upon a patient therefore results in the feature marked as the Bragg peak in graph 1.

The Bragg peak allows for a deep seated tumour to be treated whilst causing very little damage to surrounding healthy tissue. The rapid fall off of dose beyond the proton range makes proton therapy particularly well suited to tumours that are in close proximity to sensitive organs (such as the spinal cord).

The relationship between a protons energy (E) and its range (R) in tissue may be described approximately by $R_{tissue} = \left(\frac{E}{32}\right)^{1.8}$, from this, it can be estimated that energies of 220MeV would be required to treat tumours at depths of up to 30cm. To date, the acceleration of protons for medical application has been carried out using circular (rather than linear) accelerators[6].

[6]This has been attributed to our current technical abilities, and the relatively high cost-performance ratio that would be involved in accelerating protons to energies in the region of 200-250MeV using linear accelerator. Mayles, P., Nahum, A., & Rosenwald J.C. (2007) *Handbook of radiotherapy physics: theory and practice.*

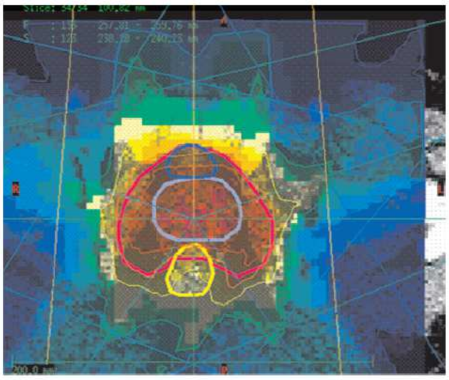
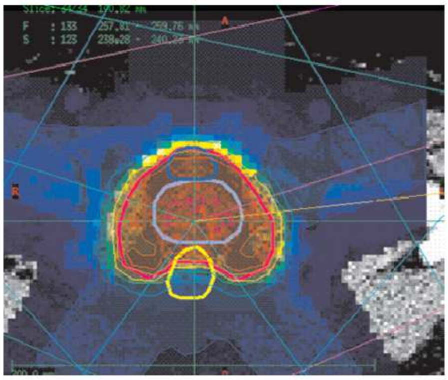
[7]

Figure 1: Above left, a simulated distribution of dose to a tumour (circled by red line) and surrounding tissue when a photon beam treatment is applied (beams entering from multiple angles in order to spread the dose to normal tissue and reduce the risk of normal tissue complications). Above right, the application of a proton based treatment to the same tumour. Blue regions are 'cold' (receive very little dose), whilst colours towards red end of spectrum indicate increased dose. It can be seen that for the proton based therapy, the higher dose regions conform more tightly to the tumour volume, leading to an overall lower dose for normal tissue.

[7] Lemoigne, Y. (2009) *Radiotherapy and Brachytherapy* [electronic book].

EXISTING ACCELERATOR BASED PROTON THERAPY UNITS

1. **The Douglas cyclotron** located at Clatterbridge Hospital (Merseyside, UK) is able to deliver 62 MeV protons for therapeutic purposes. A proton of energy 62 MeV corresponds to a range of approximately 30mm in tissue, which is adequate to treat tumours located within the eye (this is the Douglas cyclotrons current application, with the Bragg peak meaning that an ocular tumour may be treated effectively, whilst the risk of damage to the optic nerve is minimal).

   The output of the Douglas cyclotron is fixed at 62MeV which presents a problem; the Bragg peak does not necessarily occur at the most desirable depth (i.e. in the vicinity of the tumour). The solution comes in the form of perspex (a tissue equivalent material) blocks, which are introduced in to the beams path in order to ensure that the Bragg peak is found at a depth consistent with the tumour depth.

   Further to the above problem, the depths over which a tumour extends can often be of a greater range than the pristine Bragg peak (the Bragg peak due to monoenergetic particles) is able to cover, for this reason there is a need to 'spread' the Bragg peak:

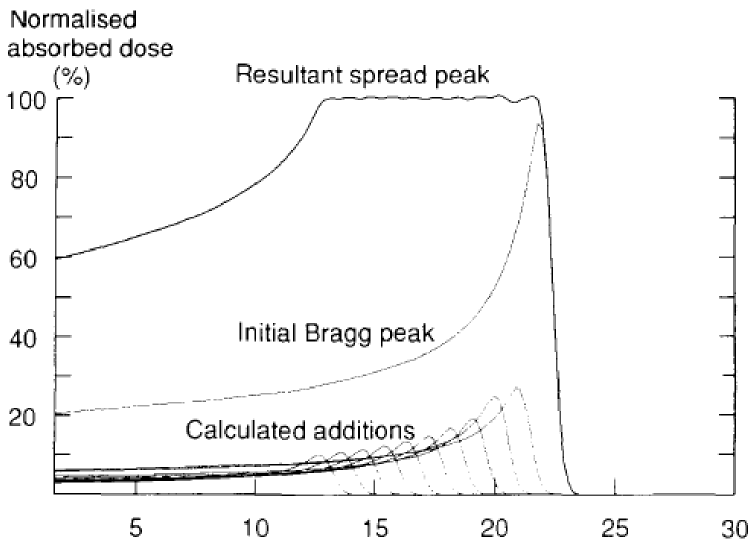

Graph 2: (Normalised dose Vs Depth) In order to effectively treat a tumour it may be necessary to spread the pristine Bragg peak.

This spreading of the Bragg peak is achieved through the use of a modulator, a perspex disc of stepped thickness which rotates through the beam line (such methods are referred to as passive scanning):

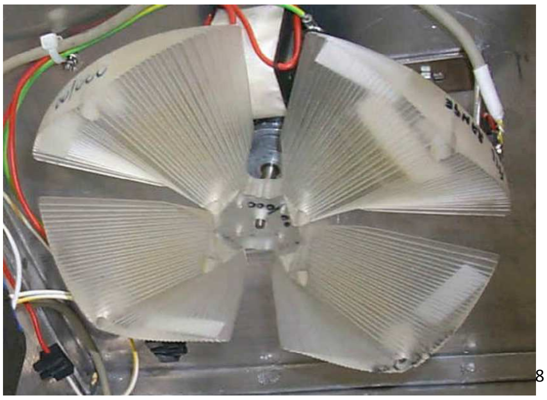
[8]

Figure 2: A perspex modulator.

2. The **Heidelberg Ion Therapy Centre (HIT)** is able to offer proton energies within the range of 48 to 221MeV, corresponding to a depth of 20 to 300mm in water[9] (as well as carbon ions[10] of up to 430MeV), for therapeutic applications. The range of energies available at the HIT are arrived at through the use of a synchrotron.

   Cyclotron design sees the orbit of a particle growing from a very small radius to a much larger radius (proportional to the particles momentum, and inversely so to the magnetic field strength), whereas within a synchrotron particles are accelerated at a fixed radius of orbit. This radius is maintained by a magnetic field which increases throughout acceleration, giving an economical advantage to the synchrotron as a result of the relative sizes of the magnetic components.

   The synchrotron provides a flexible solution that allows the HIT to deliver a range of proton energies, and for dynamic scanning to be applied[11]. However, this flexibility comes at a cost; the necessity to ramp up the magnetic field strength in maintaining the orbit radius limits the synchrotron to providing a pulsed output of relatively (when compared to a cyclotron) low intensity.

---

[8] Bonnett, D.E.et al. (1993) *The 62 MeV proton beam for the treatment of ocular melanoma at Clatterbrigde*. Available from: http://bjr.birjournals.org/cgi/content/abstract/66/790/907

[9] Mosthaf, J.M. et al. (2008) *Overview of the communication structure of the hit accelerator control system.* Available from: http://accelconf.web.cern.ch/Accelconf/pc08/papers/wep002.pdf

[10] The application of which shall not be covered here.

[11] dynamic scanning is where the beam energy is varied so that perspex blocks no longer need to be introduced into the beams path. Dynamic scanning is preferred over passive scanning as it provides better conformation of dose to a tumour.

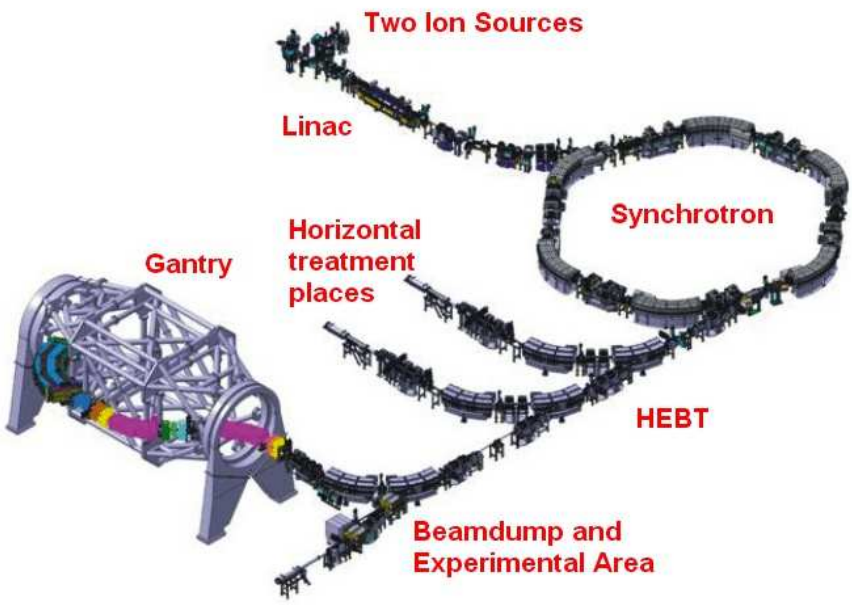

Figure 3: The Heidelberg ion therapy centre, from ion sources to treatment gantry.

Another Way: Fixed Field Alternating Gradient Accelerators (FFAG's)

FFAG accelerators were first proposed in the 1950s. Unlike for a synchrotron, the magnetic field of a FFAG accelerator is not time dependent (hence 'fixed field'), but instead varies spatially with a higher field experienced at larger radii. This means that as a particle is accelerated within a FFAG, the radius of orbit varies, but to a much smaller degree than would be expected within a cyclotron. The alternating gradient refers to periodic areas of focusing and defocusing magnetic fields which are located around the accelerator ring to provide a net focusing effect (as is the case for a synchrotron). In terms of the accelerator aspects considered important for proton therapy, FFAG's exhibit the flexibility of the synchrotron and the beam intensity of the cyclotron.

Parameter	Synchrotron	Cyclotron	FFAG
Beam Intensity	*Low*	*Plenty*	*Plenty*
Operation	*Not Easy*	*Easy*	*Easy*
Maintenance	*Normal*	*Hard*	*Normal*
Possibility of Carbon Ions	*Yes*	*Expensive*	*Yes*
Possibility of Variable Energies	*Yes*	*No*	*Yes*
Multiple Beam Extraction	*Difficult*	*No*	*Yes*

Table 1: Comparison of synchroton, cyclotron and FFAG features.

FFAG's: Scaling Vs Non-Scaling

The magnetic field of a scaling (S) FFAG increases logarithmically with orbit radius (described by $B = B_o \left(\frac{r}{r_o}\right)^k$, where k is the field index[12]), which has the advantage[13] that the shape of a particles orbit is maintained throughout acceleration. The downside to an S-FFAG is that the magnetic components are relatively large, complicated and expensive.

A FFAG design which allows for a more straightforward and compact magnetic structure is that of the non-scaling (NS) FFAG. With a magnetic field which increases linearly with orbit radius, NS-FFAG's allow the shape of a particle's orbit to vary with momentum. This variation in orbit shape could prove problematic. Resonant conditions which are usually avoided within the S-FFAG (such as integer betatron tune values (discussed in section II)) are met as a matter of course within the NS-FFAG. If resonant conditions are present for a sufficient amount of time, errors in the accelerators magnetic fields may stimulate increases in the transverse amplitudes of particles to the point that they are incident upon the accelerator wall.

[12] Edgecock, R. (2009) *FFAGs for Radiotherapy*. IOP Mayneord Phillips Summer Schools Notes.
[13] Advantages of scaling orbit described under non-scaling FFAG.

The non time dependent magnetic field means that acceleration can occur rapidly within a FFAG (the rate at which a field can be ramped up is a limiting factor within a synchrotron). It is this high rate of acceleration that allows for resonant conditions within a NS-FFAG to be passed quickly without the particle beam being lost.

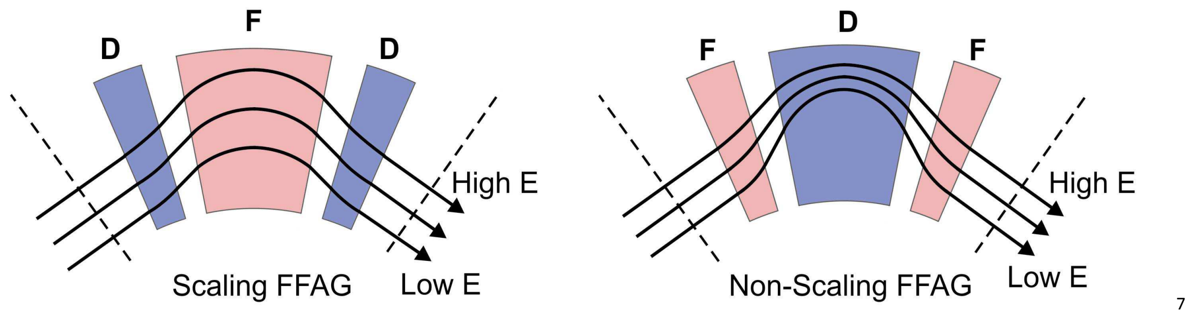

Figure 4: The NS-FFAG allows the orbit shape to vary with particle momentum, blue and red coloured areas (labelled D and F) represent alternating gradient scheme

BASROC has the aim of constructing a NS-FFAG type accelerator for the purpose of treating cancer patients through the application of proton therapy. This aim is anticipated to be realised in three steps[14]:

1. EMMA (**E**lectron **M**achine with **M**any **A**pplications) is a proof-of-principle machine which will accelerate electrons from 10.5-20.5MeV. EMMA is currently under construction at the Daresbury Laboratory (April 2010), and once completed will be used to gain better understanding of NS-FFAG design and operation.
2. PAMELA (**P**article **A**ccelerator with **ME**dica**L** **A**pplications), a 70-100MeV proton NS-FFAG prototype intended to show the practicality of the application of NS-FFAG's in the field of hadron therapy.
3. The construction of a complete facility which is able to offer proton therapy.

[14] BASROC. (2006) *British Accelerator Science and Radiation Oncology Consortium.* Available at http://www.basroc.org.uk/vision.htm

SECTION II – ACCELERATOR CONCEPTS

BEAM OPTICS

For a circular accelerator there is a clear need to affect a beam of particles in such a way that it maintains a well defined path around the circumference of the accelerator. For a beam of charged particles, their motion may be guided through the use of electromagnetic fields. The force applied to a charged particle within an electromagnetic field can be described by the Lorentz force:

$$F = q(E + v \times B)$$

For an electron of energy 20 MeV (with velocity approximately equal to the speed of light) orbiting in a circular accelerator of radius 5m, the Lorentz force required to maintain the orbit is defined as being equal and opposite to the centrifugal force:

$$F_c = \frac{mv^2}{r}$$

Which for the electron and accelerator described above, may be approximated to:

$F_c \approx \frac{\gamma m_0 c^2}{r} = \frac{E}{r}$ (a 20MeV electron is highly relativistic with a velocity very close to that of the speed of light)

$$F_c = 6.4 \times 10^{-13} N$$

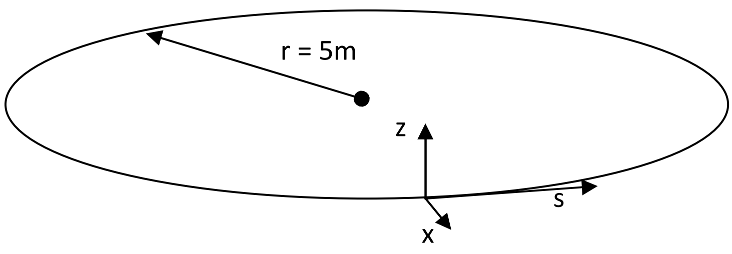

Figure 5: Definition of accelerator coordinates.

Equating with the Lorentz force gives:

$$F_L(x, z, s) = -(6.4 \times 10^{-13}, 0,0)N$$

$$\frac{F_L}{q} = (4 \times 10^6, 0,0) = E + v \times B$$

Where $q = -1.602 \times 10^{-19}$

Which may be solved (non-exclusively) by:

$E = (4 \times 10^6, 0, 0)\ Vm^{-1}$ and $B = (0, 0, 0)mT$

or

$E = (0, 0, 0)\ Vm^{-1}$ and $B = (0, -13, 0)mT$

Where $v = (0, 0, 2.998 \times 10^8)ms^{-1}$

From the formula for the Lorentz force, it may be conceived that the orbit described may be maintained by having the electron travel through an electric field of magnitude $4 \times 10^6\ Vm^{-1}$. However, the dielectric breakdown voltage of $3 \times 10^6 Vm^{-1}$ for air[15] means that such an application is unfeasible.

A magnetic field of $13\ mT$ can yield the same force as the electric field of above, but without the complications of dielectric breakdown, it is for this reason that accelerator beams are predominantly manipulated using magnets.[16]

The relationship between Lorentz force and centrifugal force can be used to define a quantity known as the magnetic rigidity:

$$F_r = -F_x$$

$$\frac{m{v_s}^2}{r} = qv_sB_z$$

$$B_z(x, z, s)r(x, z, s) = \frac{p}{q}$$

Where p is the particle momentum

The Taylor series expansion of $\frac{q}{p}B_z(x)$ gives:

$$\frac{q}{p}B_z(x) = \frac{q}{p}\left(B_{z0} + \frac{dB_z}{dx}x + \frac{1}{2}\frac{d^2B_z}{dx^2}x^2 + \cdots\right)$$

It is the first two components of this expansion that will be covered within this section, with greatest precedence put on the quadrupole field.

$\frac{q}{p}B_{z0} = \frac{1}{R}$ - Dipole equation [2.1]

$\frac{q}{p}\frac{dB_z}{dx}x = kx$ – Quadrupole equation [2.2]

---

[15] Tarr, M. (2007) *Dielectric Properties*. Available at http://www.ami.ac.uk/courses/topics/0184_dp/index.html

[16] Wille, K. (2000) *The Physics of Particle Accelerators an Introduction*. p.44

Dipole Magnets

As already detailed, for a particle travelling in the direction of the s axis, a magnetic field parallel to the z axis of the accelerator will lead to a force being experienced parallel to the x axis. It is such a field which is applied in order to bend a particle around the circumference of an accelerator. Dipole magnets may be located at intervals around an accelerator in order to provide the field necessary to maintain a particles orbit.

Quadrupole Magnets

At any point within an accelerator a particle may demonstrate a trajectory which is divergent from that of the ideal particle, without intervention such a particle would be lost. The quadrupole, an arrangement of four magnetic poles which straddle the accelerator beam pipe, serves to focus divergent particles:

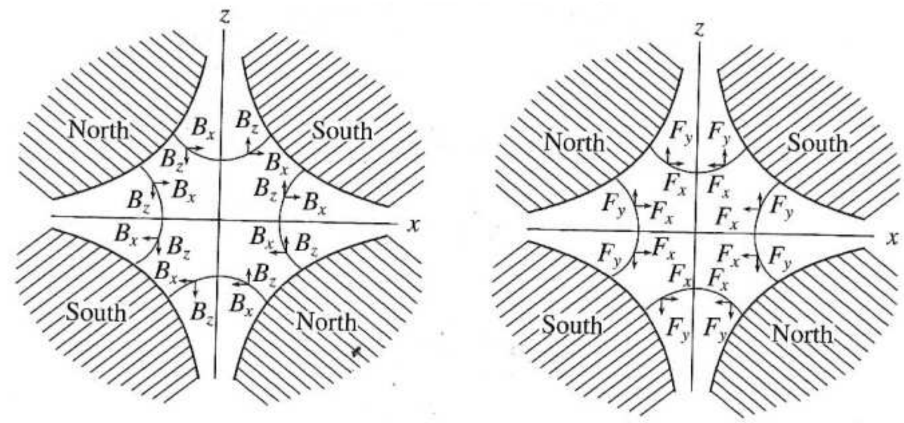

[17]

Figure 6: Sketch to show the arrangement of a quadrupole, with magnetic field and the associated force experienced by an electron (travelling into the page) marked. The orientation of this quadrupole will lead to focussing in the horizontal plane, and defocusing in the vertical plane.

The symmetries of the quadrupole mean that a particle travelling through the origin of the x-z axis shown on the diagram will experience no force, whilst the magnetic field (and so force) increases linearly with respect to displacement from the origin for an off centred particle (i.e. $\frac{dB_z}{dx} = constant$). The direction of this force is dependent upon the orientation of the quadrupole.

The quadrupole shown in figure 6 will focus a particle displaced along the horizontal axis and defocus a particle displaced along the vertical axis (when considering an electron travelling into the

[17] Wilson, E. (2001) *An introduction to particle accelerators*.

page). A rotation of the quadrupole through 90° leads to focusing in the vertical plane and defocusing in the horizontal plane.

The effect of a horizontally focusing quadrupole of length l upon a particle with initial horizontal displacement x_1 and divergence x'_1 may be described by a transfer matrix:

$$M_{QF} = \begin{bmatrix} cos\sqrt{K}l & \frac{1}{\sqrt{K}}sin\sqrt{K}l \\ -\sqrt{K}sin\sqrt{K}l & cos\sqrt{K}l \end{bmatrix}$$

Where $k = \frac{q}{p}\frac{dB_z}{dx}$

The displacement and divergence after the quadrupole (x_2 and x'_2) is given by:

$$\begin{pmatrix} x_2 \\ x'_2 \end{pmatrix} = M_{QF}\begin{pmatrix} x_1 \\ x'_1 \end{pmatrix}$$

<u>The FODO Cell</u>

The FODO cell is a commonly utilised arrangement of quadrupoles which results in a net beam focusing effect in both the horizontal and vertical plane. The FODO cell consists of a focusing quadrupole, a non-focusing region (i.e. a drift space or dipole), a defocusing quadrupole and then a second non-focusing region (**F**ocusing **0** **D**efocusing **0**).

The net focusing effect of an alternating gradient system may be demonstrated by calculating the transfer matrix for a quadrupole doublet (i.e. a defocusing quadrupole, drift space, focusing quadrupole arrangement) when approximating a quadrupole to a thin lens of length l, with focal length given by $Kl = \frac{1}{f}$:

$$M_{doublet} = \begin{bmatrix} 1 & 0 \\ -\frac{1}{f} & 1 \end{bmatrix}\begin{bmatrix} 1 & L \\ 0 & 1 \end{bmatrix}\begin{bmatrix} 1 & 0 \\ \frac{1}{f} & 1 \end{bmatrix} = \begin{bmatrix} 1+\frac{L}{f} & L \\ -\frac{1}{f^2} & 1+\frac{L}{f} \end{bmatrix}$$

Where $M_D = \begin{bmatrix} 1 & L \\ 0 & 1 \end{bmatrix}$ is the transfer matrix for a drift space of length, L.

f assumes that defocusing quadrupole is equivalent to the focusing quadrupole rotated through 90°

The resulting doublet matrix represents a thin lens with focal length $\frac{f^2}{L} > 0$[18].

[18] Edwards,D. & Syphers,M.(1993) *An Introduction to the Physics of High Energy Accelerators*

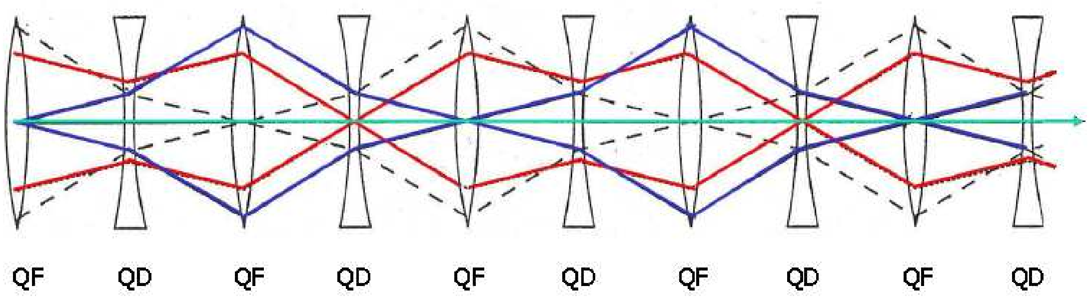

[19]

Figure 7: A number of F0D0 cells, particles with non-zero divergence are confined to the accelerator.

THE PARTICLE ACTION

An ideal particle may be regarded as one that follows the perfect path around an accelerator (i.e. does not require focusing); thinking of a particle beam as consisting of only such particles is unrealistic. In fact, at the point of injection a beam is made up of particles with a range of trajectories spread around the trajectory which would lead to an ideal orbit.

Taking into account the accelerator coordinates defined earlier, an individual particles position and motion in relation to that of an ideal particle may be described by its horizontal (x) and vertical (z) displacement as well as its horizontal $\left(x' = \frac{dx}{ds}\right)$ and vertical $\left(z' = \frac{dz}{ds}\right)$ divergence from the ideal path. The focusing effect of a F0D0 cell upon a particle with non-zero initial amplitude or divergence leads to a particle exhibiting transverse oscillations around the ideal path.

A single particle travelling through an accelerator will trace out an ellipse when the phase space coordinates x and x' (or z and z') are tracked through a number of F0D0 cells (at a specific point within each cell), the area of this ellipse will remain constant as the particle progresses through the accelerator (at a fixed value of momentum). The area of this ellipse is given by $2\pi J_x$, where J_x[20] is the action of the particle. The relationship between the maximum transverse displacement (or amplitude) and action is given by $Amplitude = \sqrt{2J_x\beta_x}$, (where β_x is given definition in the section on tune).

[19] Brandt, D. (2004) *Accelerator basics.* Available from: http://cas.web.cern.ch/CAS/Warrington/PDF/Brandt5.pdf

[20] Alexander,L. & Fetter,J.D.W.(2003) *Theoretical Mechanics of Particles and Continua*

ADIABATIC DAMPING

Liouville's theorem states that the area of an ellipse in phase space, xp_x (where p_x is the transverse momentum), will be conserved regardless of magnetic beam bending or focusing as the beam progresses along the accelerator path.

Liouville's theorem: $$Area = \oint p_x dx = constant$$

The area, $2\pi J_x$, expressed in terms of the phase space coordinates xx', will shrink with acceleration. This observation is referred to as adiabatic damping.

A conserved area in terms of J_x may be found by expressing the transverse momentum as:

$$p_x = \gamma m_o \frac{dx}{dt} = \gamma m_o \frac{dx}{ds}\frac{ds}{dt} = p_s x'$$

Where p_s is the longitudinal momentum.

The conserved area in the xx' plane is therefore given by:

$$\beta_s \gamma_s \oint x' dx = constant$$

as $p_s \propto \beta_s \gamma_s$

Where $\beta_s = \frac{v_s}{c}$, with v_s the longitudinal velocity and c the speed of light

and $\gamma = \sqrt{\frac{1}{1-\beta_s{}^2}}$

The action normalised with respect to momentum is:

$$J_{x,norm} = (\beta_s \gamma_s) J_x$$

TUNE

The betatron tune is defined as the number of complete transverse oscillations that occur each accelerator turn. For an alternating gradient accelerator the betatron tune may be defined as:

$$Q = \frac{1}{2\pi}\oint \frac{ds}{\beta(s)}$$

Where Q is the betatron tune.

and $\oint \frac{ds}{\beta(s)}$ is the change in phase of the transverse oscillation over a path length ds.

The beta function, $\beta(s)$, (also referred to as the amplitude function) defines an envelope around all trajectories of the particles travelling through a F0D0 lattice. The beta function, which is determined by the quadrupoles, varies as function of the longitudinal position, s, and for a F0D0 cell tends towards minima at defocusing quadrupoles and maxima at focusing quadrupoles (this expresses the net focusing of the F0D0 cell).

In the case of a constant gradient accelerator, the beta function is no longer dependent upon the longitudinal position, and so the tune may be given as[21]:

$$Q = \frac{1}{2\pi}\oint \frac{ds}{\beta} = \frac{R}{\beta}$$

Where R is the radius of the particle orbit.

For synchrotron design it is important that the tune does not take integer or simple fraction values as at these points error in multipole fields (as expressed in the Taylor expansion of the magnetic rigidity) can drive resonance.

[21] Wilson, E. (2001) *An introduction to particle accelerators*.

Effects of Quadrupole Alignment Errors

A quadrupole misaligned from the beam axis $(x = z = 0)$ of an accelerator by $(\Delta x, \Delta z)$ (as shown in figure 5) will lead to particles experiencing a dipole type field error. The strength of the field is related to the quadrupole displacement by:

$\begin{pmatrix} \Delta B_x \\ \Delta B_z \end{pmatrix} = g \begin{pmatrix} \Delta z \\ \Delta x \end{pmatrix}$ where g is the quadrupole gradient $\frac{dB_z}{dx}$

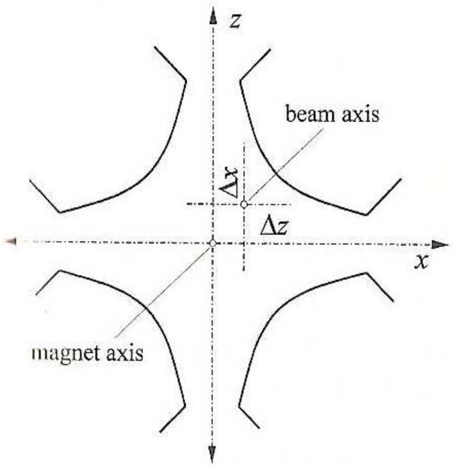

[22]

Figure 8: An off centred quadrupole.

For a short quadrupole (longitudinal length l) the effect of the dipole field errors influence may be approximated to a single angular 'kick' (with no instantaneous change in amplitude) at the midpoint $(l/2)$ of the quadrupole. The nature of this kick is given by:

$$\begin{pmatrix} \Delta x' \\ \Delta z' \end{pmatrix} = \frac{q}{p} \begin{pmatrix} \Delta B_z \\ \Delta B_x \end{pmatrix} l$$

[22] Wille, K. (2000) *The Physics of Particle Accelerators an Introduction.*

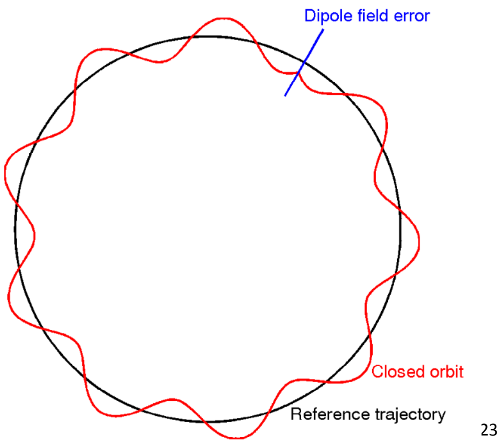

Figure 9: Showing a closed orbit distortion due to a dipole field error.

Considering a particle with zero initial offset of amplitude and trajectory relative to the ideal beam path, $(x, x') = (0,0)$, the amplitude and trajectory just after a kick is given by $(x, x') = (0, \Delta x')$. This new trajectory will, as the particle progresses longitudinally, give an increase in the transverse displacement, and with subsequent focusing lead to transverse oscillations.

If the betatron tune is of an integer value, then the dipole field error kick due to the misalignment of a quadrupole will add coherently each accelerator turn. This means that over a number of turns the amplitude of the transverse oscillation will be increased, and for a sufficiently large number of turns beam particles will be incident upon the accelerator wall.

However, if the betatron tune is of a non-integer value, then the dipole field error kicks of each accelerator turn will add incoherently and over a number of turns there will be no net change in the transverse oscillation amplitude.

[23] Wolski, A. (2006) *Effects of Linear Imperfections.* Linear Dynamics lecture notes. Available at http://pcwww.liv.ac.uk/~awolski/Teaching/LinearDynamics/LinearDynamics-Lecture10.pdf

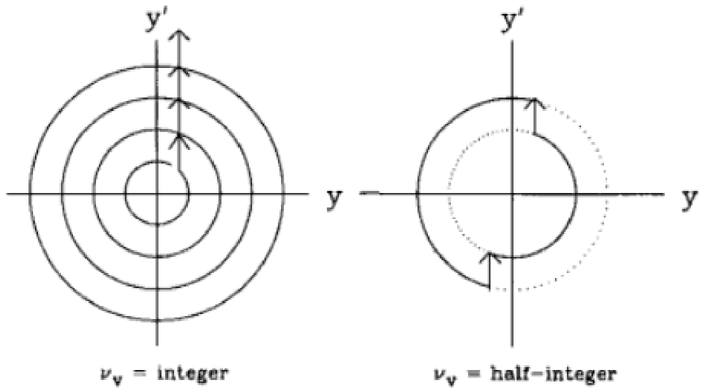

[24]

Figure 10: For integer tune (left) the amplitude grows upon each accelerator turn, for half integer tune (right) there is no net amplitude growth over a number of turns.

[24] Lee, S.Y. (2004) *Accelerator physics.*

Section III – Simulation

Aims

- To develop a computer model, based on the EMMA accelerator, which is able to simulate the increase in transverse amplitude due to integer tune crossing.
    - To construct the model on the premise that an alternating gradient accelerator may be approximated to a constant gradient accelerator for the purpose of investigating transverse amplitude growth.
- To use the developed model to examine the effects of acceleration rate transverse amplitude growth.
- To compare the output of this model to the output which uses a 'full physics' approach to describing the transverse motion.

N.B. 'full physics' refers to a model for which the behaviour of a particles transverse motion at a given time is dependent upon the accelerator component in which the particle is located (i.e. the lattice is not approximated to a constant gradient). The exact model to be used for comparison is that presented by S.Machida in the paper '*Resonance Crossing and Dynamic Aperture in Non-scaling Fixed Field Alternating Gradient Accelerators'*, an outline of which may be found in the appendix.

The EMMA Lattice

EMMA is the proof of principle linear NS-FFAG accelerator upon which this simulation shall be based.

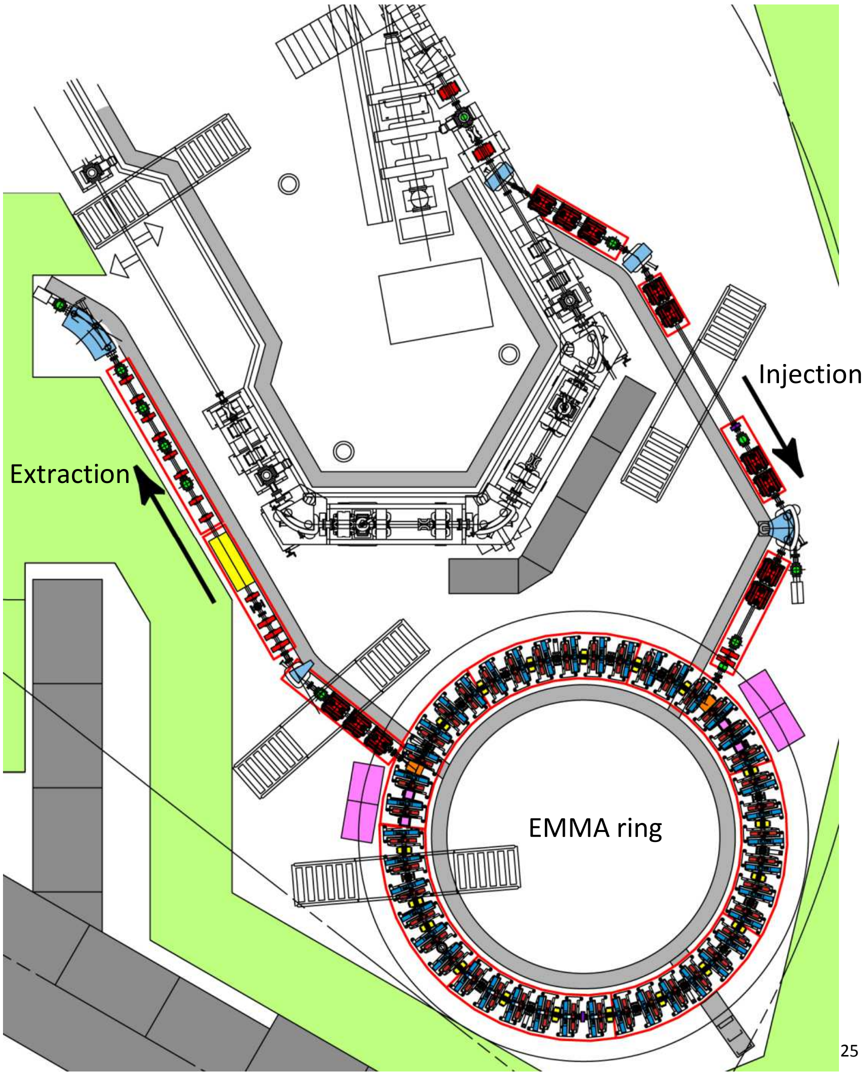

[25]

Figure 11: Schematic of the main EMMA ring as well as injection component from ALICE and extraction line.

In considering the guidance and focusing components of EMMA the accelerator ring may be divided into 42 periodic F0D0 cells. The quadrupole magnets within EMMA are combined function, with each magnet aligned off centre in order to provide a dipole field component for bending particles around the ring, and a quadrupole field component for focusing a divergent beam.

The values used in the simulation to define the lattice may be found in the appendix.

[25] Conform. (2007) *EMMA layout phase 2*. Available at: http://www.conform.ac.uk/documents/emma/dwg-drawings/207-10324-C-EMMA-LAYOUT-PHASE-2-colour.jpg

MODEL APPROXIMATIONS

Some of the approximations to be made in the production of the model of EMMA are:

1. The transverse motion of the NS-FFAG may be treated approximated to that of an accelerator with a constant field gradient.
2. The Transverse Motion Along the z Axis may be Modelled Independently.
3. Electrons are accelerated from 10.75MeV to 20.75MeV, where acceleration is represented by a constant energy increase at each cell.
4. The time take to complete one orbit is constant through acceleration.
5. The lognitudinal velocity is equal to the speed of light.

1. Constant Gradient Aprroximate Model

The transverse motion of a particle travelling through an accelerator may be described by Hill's equation:

$$\frac{d^2z}{ds^2} + K(s)z = 0 \qquad [3.1]$$

and

$$\frac{d^2x}{ds^2} + K(s)x = 0$$

Where K is dependent upon which component is being traversed within an alternating gradient accelerator, and is in the form of equation [2.2] for a quadrupole.

The repeating cell arrangement of EMMA means that K is periodic, so that:

$$K(s + c) = K(s) \qquad [3.2]$$

Where here c may represent the length of a cell.

A primary aim of this project is to explore the notion that for a lattice with known tune values, the transverse motion may be described approximately by the equation:

$$\frac{d^2z}{dt^2} + \omega^2 z = 0 \qquad [3.3]$$

Where

$$\omega = \frac{2\pi Q_z}{T_o}$$

With Q_z being the betatron tune for the vertical axis

T_o being theorbit time for a particle in the accelerator.

This approximation effectively treats the focusing effect of an alternating gradient lattice as a constant gradient spanning the enitre circumference of the accelerator, and describes particle motion as sinusoidal around the ideal beam path (in the fashion of a simple harmonic oscillator), rather than as the more complex motion shown in figure 7. The constant gradient representation would see equation [3.1] interpreted as:

$$\frac{d^2z}{ds^2} + Kz = 0 \quad [3.4]$$

i.e. K is still dependent upon the momentum of the particle, but no longer dependent upon the longitudinal position 's'.

By rearranging these simple harmonic motion type equations [3.3] and [3.4], it can be seen that the restoring force may be taken as

$$F_z = \frac{d^2z}{ds^2} = -Kz$$

and the acceleration as

$$a_z = \frac{d^2z}{dt^2} = -\omega^2 z$$

Relating through $F = ma$, gives the relationship between K and ω as:

$$K = m\omega^2$$

2. The Transverse Motion Along the z Axis may be Modelled Independently

This is the approximation that amplitude growth in the direction of the z axis may be simulated without consideration of the amplitude growth along the x axis. This leads to a simplified model, and a reduction in the amount of computer time required for simulations. This is may be a valid approximation if the average velocity along the x axis is a fraction of the longitidunal (s axis) velocity. It is the transverse motion in the vertical (z) axis that is to be simulated as for a FFAG this has the smaller aperture, also the behaviour of transverse motion along the vertical axis should be representitive of transverse motion for the horizontal axis.

3. Energy Range of 10.75 MeV to 20.75 MeV with Acceleration Represented by a Constant Energy Increase at Each Cell

The acceleration range of 10.75 MeV to 20.75 MeV differs from the acceleration range of EMMA (10.5 MeV to 20.5 MeV), but is in keeping with the 'real physics' model with which results from this simulation will be compared. A small increase of 0.25 MeV in injection energy keeps the initial horizontal and vertical tune away from integer values.

The representation of acceleration as a constant energy increase at each cell (rather than simulating the effects of rf cavities every other cell) is a simplification which should result in a reduction in the amount of time each simulation takes to run. Once again, this is in keeping with the 'real physics' model, for which, this representation of acceleration also eliminates the effects due to longitudinal and transverse coupling[26].

4. Constant Time of Flight

For the purpose of this simulation, the time taken for an electron to complete one turn in EMMA will be regarded as being constant with energy, and is to be defined by the circumference of EMMA divided by the speed of light (i.e. independent of the amplitude of transverse motion).

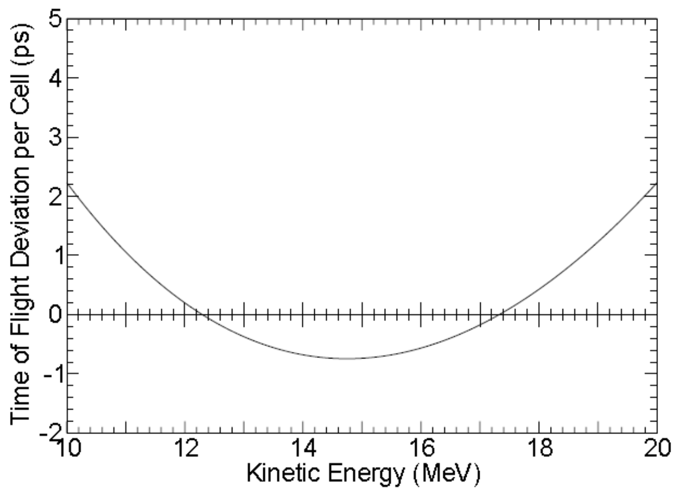

[27]

Graph 3: Time of flight is approximately isochronous within the range of acceleration.

[26] For a model in which the time taken for one accelerator turn is dependent upon the transverse amplitude of a particle, it is possible that a particle with a sufficiently large transverse amplitude will enter into the decelerating phase of the rf. Representing acceleration as a constant increase in energy per cell isolates this problem from that of particle loss due to resonance.

[27] Berg, J. (2007) *The EMMA Experiment.*

The NS-FFAG accelerator lattice is designed so as to give a parabolic variation in orbit length during acceleration (with the minimum of the parabola located at the median particle energy). Referring to graph 5, the range in time of flight deviation per cell, $\mathbf{3}\boldsymbol{ps}$, is small compared to the time of flight per cell, which is approximately $\mathbf{1.3}\ \boldsymbol{ns}$ (for a particle with orbit length of 16.57 m and velocity close to the speed of light).

When considering the time of flight dependency on transverse amplitude, the relative differences between the wavelength of the transverse oscillations and the transverse amplitude may be taken into account. The shortest wavelength (λ) of vertical transverse oscillation within EMMA is 1.3m; the maximum vertical transverse amplitude (A) (limited by the vertical aperture in the focusing quadrupole) is 8.9mm. An estimation of the maximum difference in path length between a zero amplitude particle and a high amplitude particle is obtained by approximation of the path length between the maximum and minimum of the oscillation to being the hypotenuse of a triangle with sides 2A and λ/2:

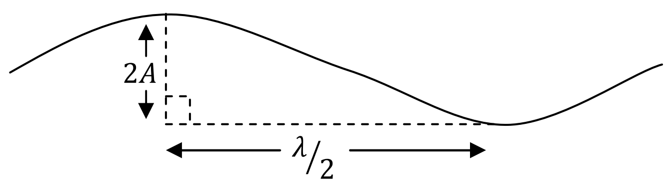

Figure 12: Estimation of path length for a high transverse amplitude particle in EMMA.

This method shows an increase in path length of 0.04% of the straight through path for a high amplitude particle.

5. <u>Longitudinal Velocity Equal to the Speed of Light</u>

For the electron energy range of 10.75 MeV to 20.75 MeV there is a $\mathbf{8} \times \mathbf{10^{-4}}\ \boldsymbol{c}$ (where $\boldsymbol{c}$ is the speed of light) increase in speed, and a maximum deviation in speed from the speed of light of $\mathbf{1} \times \mathbf{10^{-3}}\boldsymbol{c}$ (a difference of 0.1%).

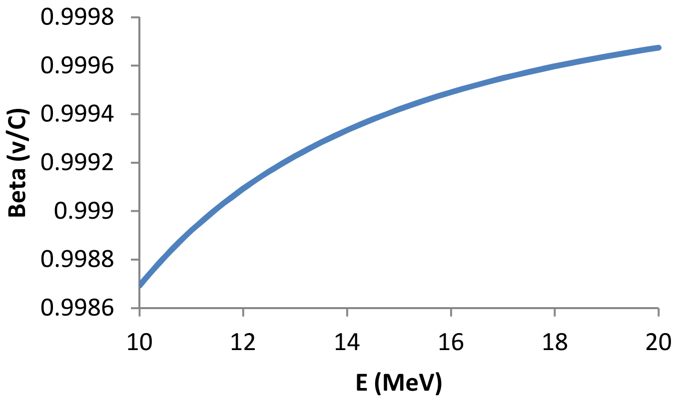

Graph 4: Beta Vs Energy for EMMA's acceleration range

The speed of the particle is given by $\sqrt{{v_x}^2 + {v_z}^2 + {v_s}^2}$, the assumption is made that $v_s \gg \sqrt{{v_x}^2 + {v_z}^2}$ (from this it follows that the Lorentz force due to transverse velocity will be relatively small).

Amplitude Growth of a Single Particle

A solution to the simple harmonic motion equation of [3.3] comes in the form of:

$z = A cos(\omega t + \varphi)$

Which may be rewritten using the trigonometric identity

$cos(x + y) \equiv cos(x)cos(y) - sin(x)sin(y)$ to give:

$z = Acos(\omega t) + Bsin(\omega t)$ [3.5]

The velocity of a particle at a time, t, is then given by:

$v = \frac{dz}{dt} = -\omega Asin(\omega t) + \omega Bcos(\omega t)$ [3.6]

and the coefficients A and B are found by setting $t = 0$.

At $t = 0$, $z_i = A$

$v_i = \omega B$

(where the subscript 'i' denotes initial)

Substituting into [3.5] and [3.6] gives

$z = z_i cos(\omega t) + \frac{v_i}{\omega} sin(\omega t)$

$v = -\omega z_i sin(\omega t) + v_i cos(\omega t)$

Which may be used to create a transfer matrix for transverse displacement and velocity through a time t:

$$\begin{pmatrix} z \\ v \end{pmatrix} = \begin{pmatrix} cos(\omega t) & \frac{1}{\omega} sin(\omega t) \\ -\omega sin(\omega t) & cos(\omega t) \end{pmatrix} \begin{pmatrix} z_i \\ v_i \end{pmatrix} \qquad [3.7]$$

This transfer matrix will be used to estimate (under the constant gradient approximation) the transverse amplitude and velocity of a particle at intervals consistent with the location of individual quadrupoles.

The transverse amplitude is then given by:

$A_z = \sqrt{z^2 + \left(\frac{v_z}{\omega}\right)^2}$

All particles within the simulation are started with 0mm initial amplitude.

The main features of the Matlab code for doing this are annotated below (in red):

```
for c1 = 1:(CT-1),
```

1. **Loop runs over the total number of cells traversed during acceleration, i.e. for acceleration over 100 turns, CT=100*42**

```
  energy = Estart + c1*deltaE;
  tune = (0.0549*energy^2) - (2.4572*energy) + 32.4479;
  freq = tune / T0;
  wb = 2*pi*freq;
```

2. **Energy and tune (frequency) parameters unique to each cell.**

```
  dvF = (F(c,3) * LightSpeed * Q(2,1))/(energy*1e6*qe); %transverse
velocity kick at focussing quad
  dvD = (F(c,4) * LightSpeed * Q(2,2))/(energy*1e6*qe); %transverse
velocity kick at defocussing quad
```

3. **Gives transverse focusing and defocusing velocity kicks based upon misalignment of current cell.**

```
vector1 = [x1(c1)
           v1(c1)];
```

4. **Initial transverse displacement and velocity, based upon displacement and velocity at midpoint of defocusing quadrupole in previous cell (after kick), or if c1=1, upon the injection conditions.**

```
  M = M1(wb, TDF);
```

5. **Gives transfer matrix specific to the angular frequency of the particle and to the time taken for the particle to travel from the midpoint of the defocusing quadrupole in the previous cell, to the midpoint of the focusing quadrupole in the current cell.**

```
  vector2 = M * vector1;   %travel from middle previous defocussing quad to
middle of following focussing quad
  vector2(2)=vector2(2) + dvF; %adds kick from horizontally focussing quad
to vector
```

6. **Estimates transverse displacement and velocity (based upon constant gradient approximation) of particle at midpoint of focusing quadrupole, and adds transverse velocity kick.**

```
  M = M1(wb, TFD);
  vector2 = M * vector2;  %travel from previous focussing quad to following
defocussing quad
  vector2(2)=vector2(2) + dvD; %adds kick from horizontally defocussing
quad to vector
```

7. **Carries out steps 5 and 6 for the defocusing quadrupole (based on time taken for particle to travel from midpoint of focusing quadrupole to midpoint of defocusing quadrupole.**

```
  x1(c1+1) = vector2(1);
  v1(c1+1) = vector2(2);
```

8. **Sets initial transverse displacement and velocity for next cell.**

```
  A1(c1+1) = sqrt(x1(c1+1)^2 + (v1(c1+1)^2 / wb^2));
  beta1(c1+1) = L/(2*pi*tune);
```

9. **Calculates amplitude and betatron function.**

```
  c = c+1;
  if c>42
      c=1;
```

```
    end
      10. For loop counts through cells, and repeats after 42 (i.e. one revolution).
end
```

Plots of single particle amplitude Vs tune are presented in the form of $\sqrt{2J_z}$ Vs tune to aid comparison with the real physics model.

The transverse displacement, z, is related to $\sqrt{2J_z}$ by:

$$z = \sqrt{2J_z\beta_z}cos\varphi_z$$

z is a maximum when $cos\varphi_z = 1$, which gives the amplitude of the oscillation along the z axis as:

$$A_z = \sqrt{2J_z\beta_z}$$

$$\sqrt{2J_z} = \frac{A_z}{\sqrt{\beta_z}}$$

With the approximation of an alternating gradient accelerator to a constant gradient accelerator the beta function, β_z, is longitudinally invariant. β_z, given as a function of particle energy is:

$$\beta_z = \frac{R}{Q_z(E)}$$

where R is the radius of the particle orbit

$Q_z(E)$ is the vertical tune at energy 'E'.

The plot of $\sqrt{2J_z}$ Vs tune for no perturbing influence and a starting displacement of 1mm is as follows, the effects due to adiabatic damping are not applicable (which is contrary to the output of the real physics model):

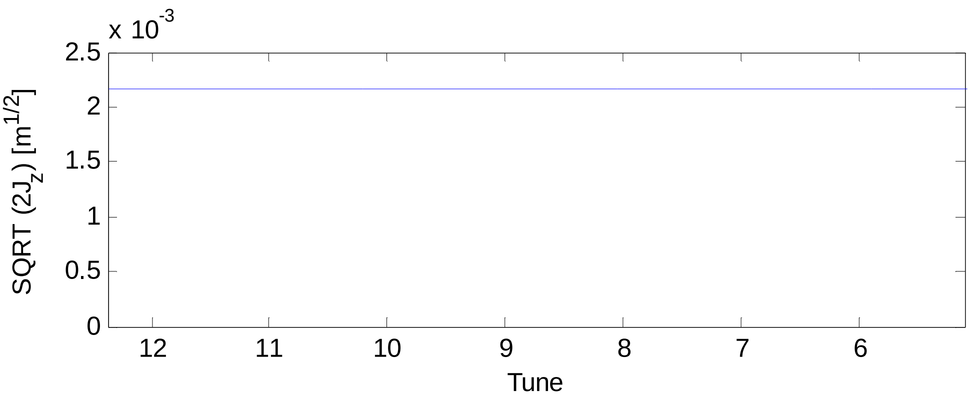

Graph 5: Start amplitude of 1mm and standard deviation of alignment error magnitudes of 0m.

Introduction of Quadrupole Alignment Errors

The alignment errors to be considered are for the offsetting of the cell position (the focusing and defocusing quadrupole within cell are equally misaligned) into the x-z plane, the magnitude of the errors are assumed to be of a Gaussian nature with a 2σ cut off.

The Gaussian probability density function is given by:

$$P(\Delta R) = \frac{1}{\sigma\sqrt{2\pi}} \exp\left(\frac{-(\Delta R - \mu)^2}{2\sigma^2}\right)$$

Where $P(\Delta R)$ is the probability of an error of a value ΔR

μ is the mean

σ^2 is the variance

The magnitude of the quadrupole alignment error is produced using the Matlab 'randn' function, values obtained falling outside of the 2σ range are reevaluated:

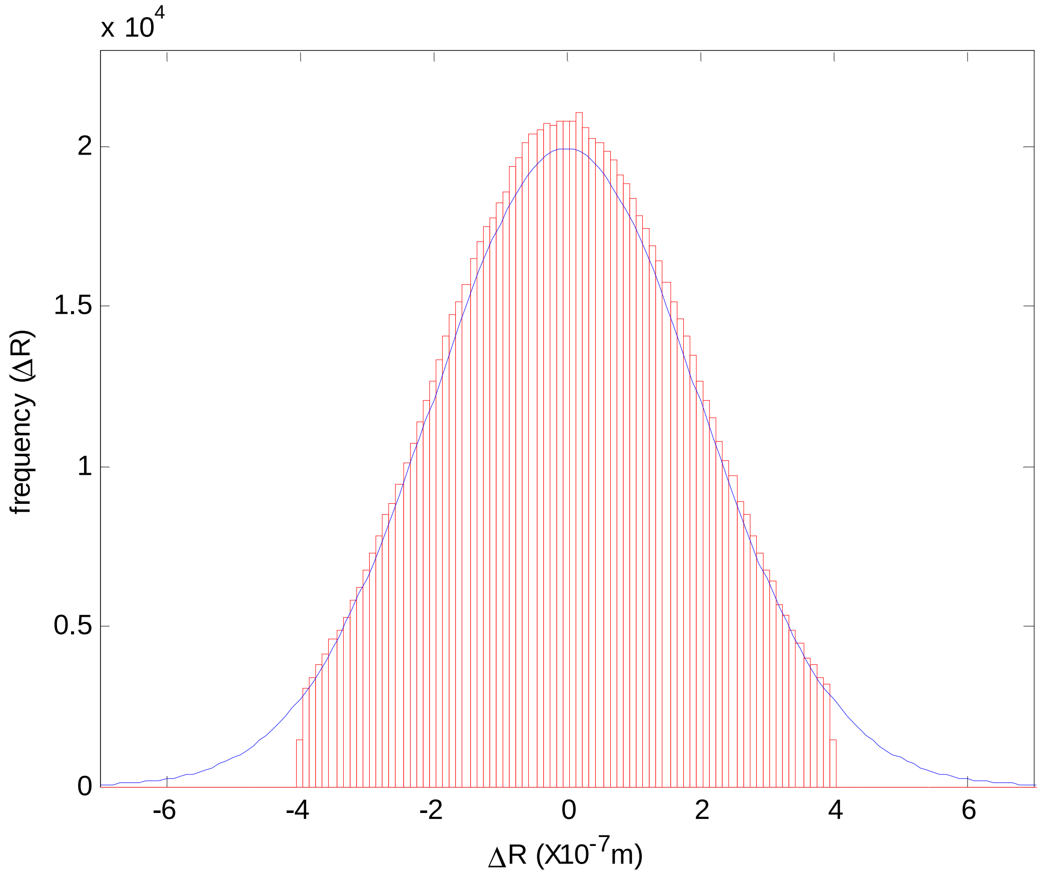

Graph 6: Blue line showing the Gaussian probability distribution for μ=0 and σ=2x10^{-7}m. Red histogram showing the result of 1x10^{6} trials based on the same parameters as for the probability distribution (blue line), and with outcomes of $|\Delta R| > 2\sigma$ re-trialled.

A direction is then assigned to the error using the Matlab ‘rand’ function (which generates a pseudo-random number in the interval 0-1), through $\theta = rand * 2\pi$.

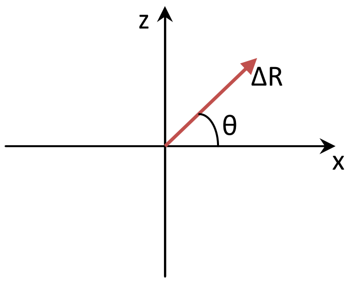

$$\Delta R_x = \Delta R\ cos\vartheta$$

$$\Delta R_z = \Delta R\ sin\vartheta$$

Figure 13: Alignment is offset at a random angle into the x-z

The distribution of quadrupole alignment errors along the z axis (the axis for which amplitude growth will be considered) is as follows:

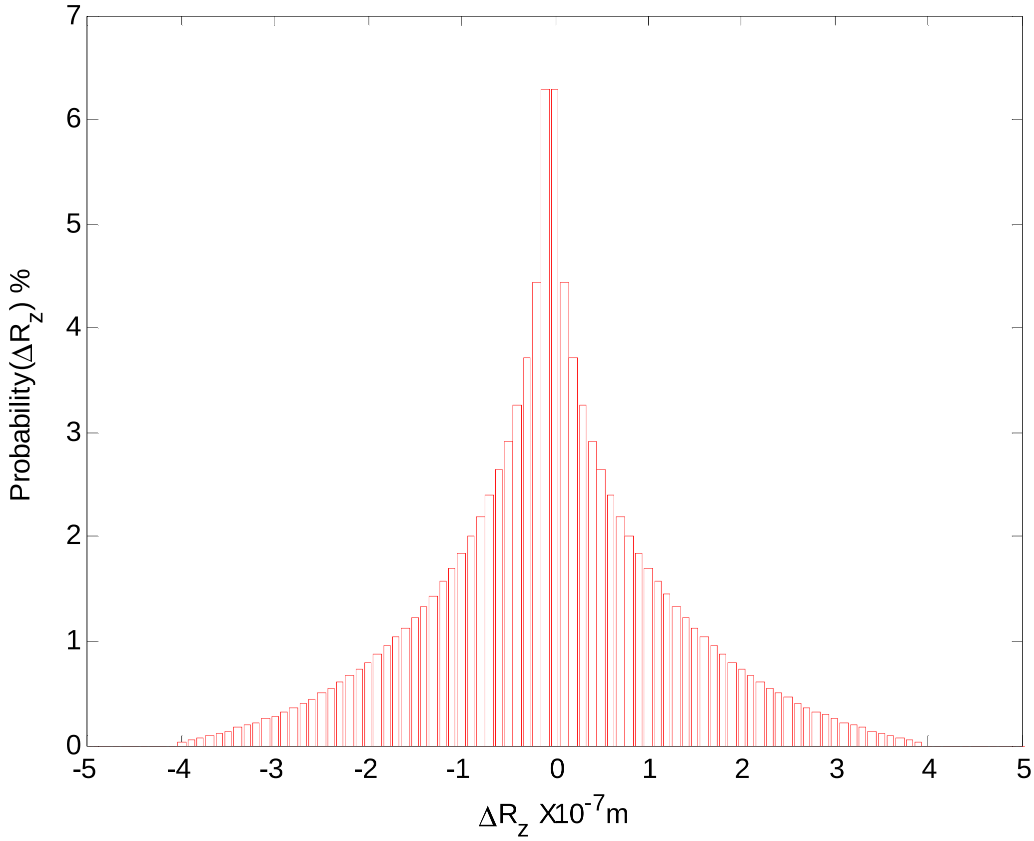

Graph 7: Showing the distribution of errors in quadrupole alignment along the z axis. Generated by $1x10^6$ trials.

When studying the amplitude growth of a single particle a 42 element array is produced to contain the magnitudes of cell alignment errors. Random number seeds (to determine the set of pseudo-random numbers utilised) are used in order to provide direct comparison between different rates of acceleration. Below is the set of cell alignments used to produce graph 10 ($\sqrt{2J_z}$ Vs tune):

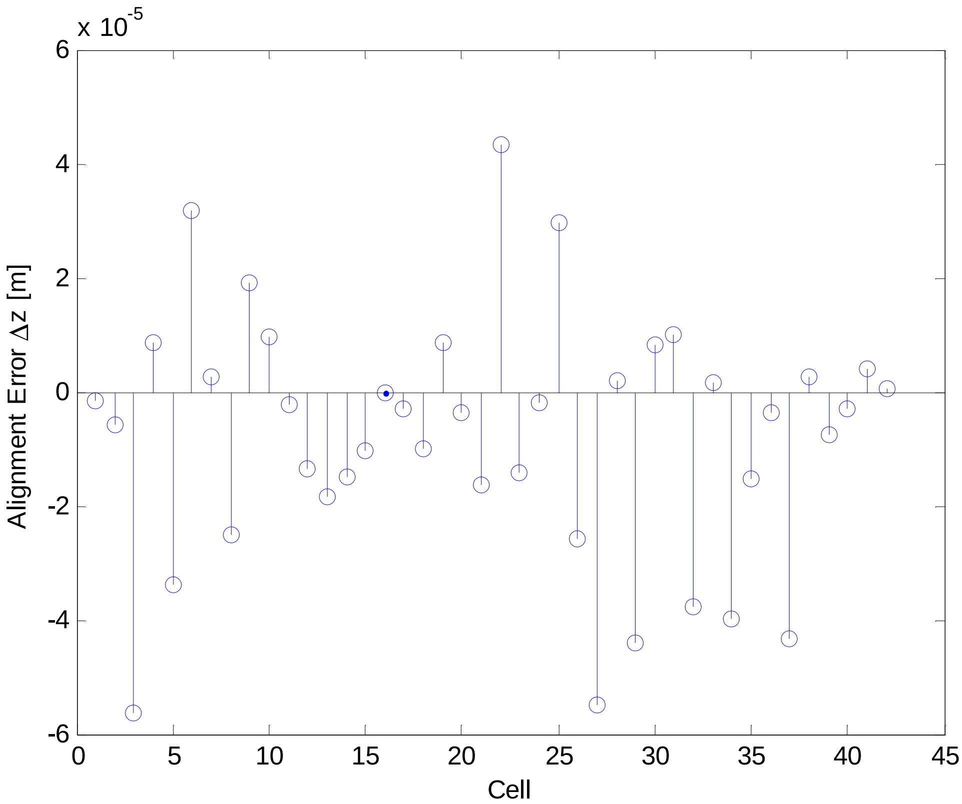

Graph 8: Quadrupole alignment errors in z direction as utilised in simulation for graphs Seed number 788.

The effect of a misaligned quadrupole may be seen as a kick in the transverse velocity, which is given by the Lorentz force:

$F = q(v \times B)$

For an error in the quadrupole alignment along the z axis, the Lorentz force is given by:

$F_z = qv_s \frac{dB_x}{dz} \Delta z$ (3.8)

Which leads to the acceleration of the particle along the z axis:

$F_z = m \frac{dv_z}{dt}$ (3.9)

Where m is the relativistic mass, $m = \gamma m_o = \frac{E}{c^2}$

The transverse velocity kick is defined by equating (3.8) and (3.9):

$$dv_z = \frac{F_z}{m}dt = \frac{qv_s}{m}\frac{dB_x}{dz}\Delta z dt$$

And is applied at the midpoint of a misaligned quadrupole:

$$v_{z,f} = v_{z,i} + dv_z$$

Where

$v_{z,f}$ is the transverse velocity after the kick

$v_{z,i}$ is the transverse velocity before the kick

Effect of the Standard Deviation of Quadrupole Misalignment on Amplitude Growth

It can be expected that the extent of transverse amplitude growth at integer tune values is related to the magnitude of the standard deviation of quadrupole alignment errors. In order to test this proposition, simulations were carried out for quadrupole alignment errors of standard deviations ranging from 0.2μm to 100μm (at intervals of 0.2μm). For each value of standard deviation a unique pattern of quadrupole alignment errors was created, a particle (with zero initial transverse amplitude) was then accelerated from injection energy to extraction energy and the maximum transverse amplitude throughout acceleration recorded. A total five hundred error patterns was selected so as to reduce statistical errors when finding a line of best fit. For all simulations (unless otherwise stated), particles start with zero transverse displacement and velocity, any non-zero amplitude found during acceleration is therefore as a result of growth due to quadrupole misalignments.

A plot of maximum amplitude Vs standard deviation was found to be as follows:

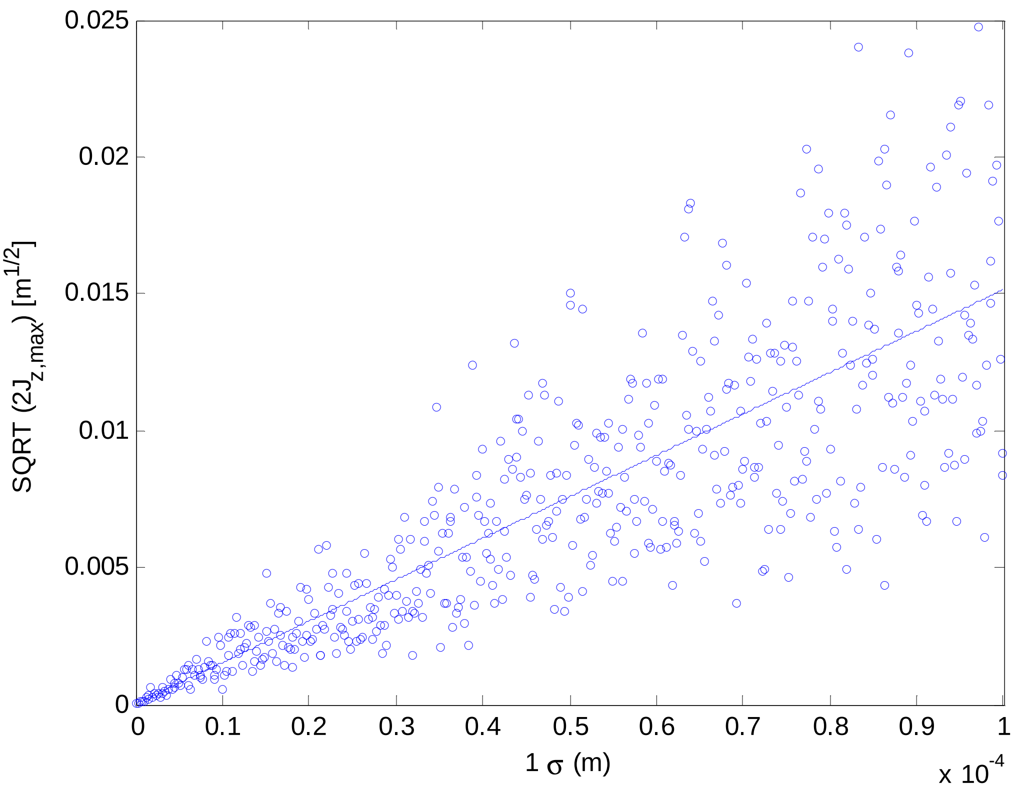

Graph 9: Plot of maximum amplitude Vs standard deviation for acceleration over 100 turns, line of best fit generated using the Matlab polyfit function.

Rate of Acceleration

The number of accelerator turns for which resonant conditions may lead to amplitude growth is dependent on the number of turns over which accelertion occurs, with slow acceleration rates leading to stronger amplitude growth at integer tune values. Insight into the importance of the rate of acceleration may be gained visually bycomparing plots of $\sqrt{2J_z}$ Vs Tune for regimes identical in all but the number of turns over which acceleration occurs:

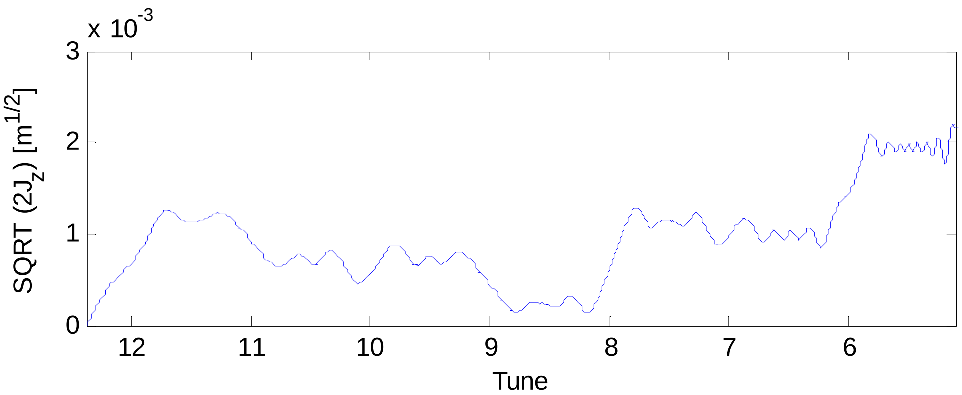

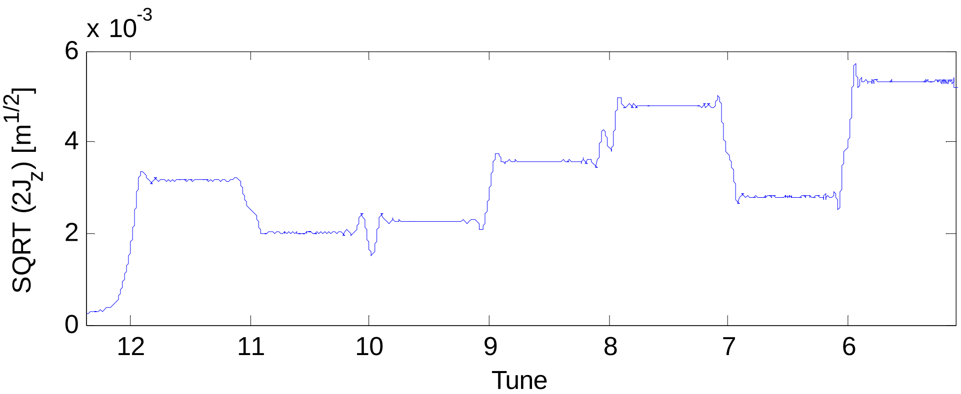

Graph 10: Top acceleration through 100 turns, bottom acceleration through 1000 turns. Both plots completed using the same pattern of quadrupole alignment errors (standard deviation of 30µm).

In order to gain a quantitative appreciation of the effects of the acceleration rate, the simulations completed in order to produce graph 9 (maximum amplitude Vs standard deviation) are repeated for a range of acceleration rates (acceleration over 100, 200, 300, 400, 500, 750, 1000, 1500 and 2000 turns). Below is a plot showing maximum amplitude Vs standard deviation for samples of acceleration over 100 and 1000 turns:

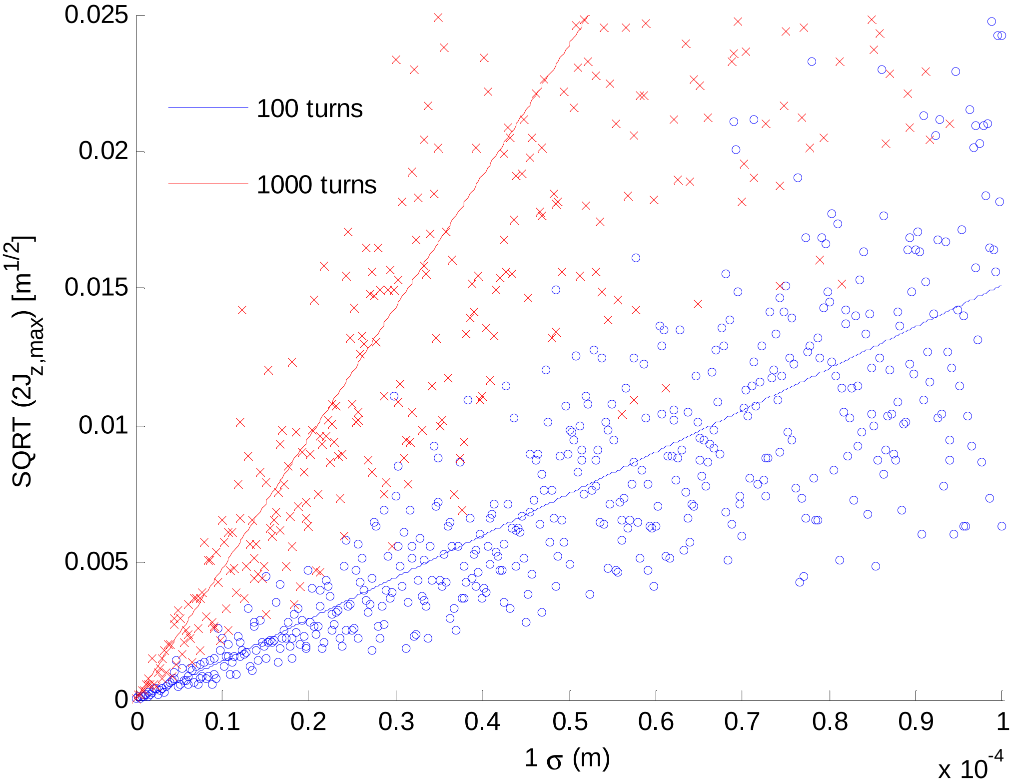

Graph 11: Transverse amplitude Vs Standard deviation of alignment error for acceleration through 100 turns and 1000 turns, completed for 500 different values of standard deviation (each representing a different pattern of alignments).

For each rate of acceleration a line of best fit (in the form of $y = mx + c$) for the data of maximum amplitude Vs standard deviation is produced using the Matlab polyfit function. A graph of the gradient of each line of best fit, $\Delta\sqrt{2J_{z,max}}\big/\Delta\sigma$, is then plotted as a function of the rate of acceleration.

The error on each value of $\Delta\sqrt{2J_{z,max}}\big/\Delta\sigma$ is based upon the distribution of the points of $\sqrt{2J_{z,max}}$ around the line of best fit, and is calculated by[28]:

$$\sigma_m = \sqrt{\frac{\chi^2}{(N-2)}}\sqrt{\frac{N}{N\sum_{i=1}^{N} x_i{}^2 - \left(\sum_{i=1}^{N} x_i\right)^2}}$$

Where,

N is the number of points

[28] Press, W.H. et al. (1995) *Numerical Recipes in C*

x_i is the standard deviation of an alignment error

The χ^2 value is given by:

$$\chi^2 = \sum_{i=1}^{N} \left(\frac{y_i - (mx_i + c)}{\sigma_i} \right)^2$$

Where,

y_i is an individual measured point (in this case a value for maximum amplitude obtained through simulation)

$mx_i + c$ is the value of y_i as determined by the line of best fit

σ_i is the error on the individual point

In determining the error on the gradient each value for maximum amplitude is treated with equal weighting ($\sigma_i \equiv 1$).

$\Delta\sqrt{2J_{z,max}}/\Delta\sigma$ plotted as a function of the rate of acceleration:

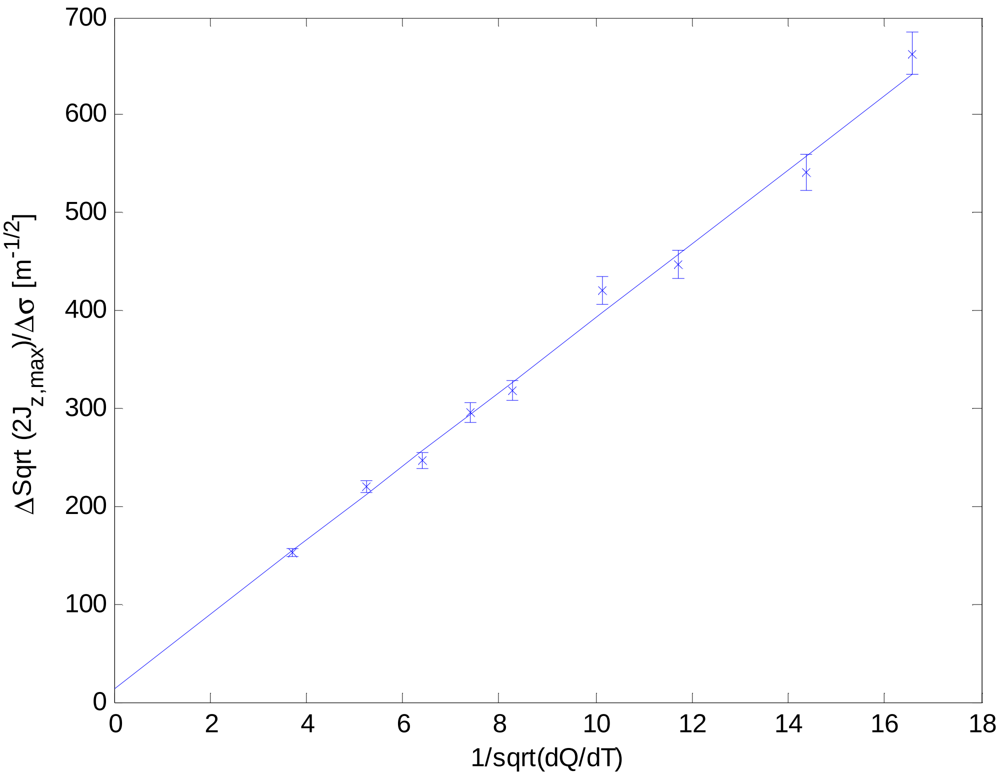

Graph 12: Amplitude growth as a function of the rate of acceleration.

$1\Big/\sqrt{dQ/dT}$ is the inverse of square root of the tune change per turn, and is chosen so that data points sit on a straight line (in keeping with figure 4 of Machida (2008)). In calculating dQ/dT the tune is described as varying linearly with the number of turns, so that:

$$dQ/dT = \frac{Maximum\ Tune - Minimum\ Tune}{Number\ of\ Turns}.$$

The gradient describing a line of best fit to the points of graph 12 is found as that which minimises the χ^2 function $\left(\partial\chi^2/\partial m = 0 \quad where\ m\ is\ the\ gradient\right)$[29].

$$m = \frac{SS_{xy} - S_x S_y}{\Delta}$$

$$\sigma_m = \sqrt{\frac{S}{\Delta}}$$

Where the individual terms are defined as:

$$S \equiv \sum_{i=1}^{N} \frac{1}{\sigma_i{}^2} \qquad S_{xy} \equiv \sum_{i=1}^{N} \frac{1}{\sigma_i{}^2} \qquad S_x \equiv \sum_{i=1}^{N} \frac{x_i}{\sigma_i{}^2} \qquad S_y \equiv \sum_{i=1}^{N} \frac{y_i}{\sigma_i{}^2}$$

$$\Delta \equiv SS_{xx} - S_x{}^2 \qquad S_{xx} \equiv \sum_{i=1}^{N} \frac{x_i{}^2}{\sigma_i{}^2}$$

The gradient obtained for the amplitude growth as a function of acceleration rate was:

$$\frac{\Delta\left(\Delta\sqrt{2J_{z,max}}\Big/\Delta\sigma\right)}{\Delta 1\Big/\sqrt{dQ/dT}} = (38 \pm 1\,)m^{-1/2} \text{ (3\% error)}$$

With the fit giving a χ^2 per number of degrees of freedom as 1.27.

[29] Press, W.H. et al. (1995) *Numerical Recipes in C*

THE PHYSICAL APERTURE

The physical aperture was defined as the minimum initial amplitude (for a particular rate of acceleration and distribution of quadrupole alignment errors) for which a particle was not accelerated to the extraction energy as a result of the particle being incident upon an accelerator component.

Within the simulation particles with $\sqrt{2J_z}$ of more than $19.3mm^{-1/2}$ were considered to have been lost, this is consistent with the transverse amplitude of a particle being more than half the aperture of the smallest aperture component (this is for the focusing quadrupole which has a vertical aperture of 17.8mm).

Five hundred different values of the standard deviation of quadrupole misalignment are evaluated for two different rates of acceleration (through 100 and 1000 turns).

For each combination of standard deviation and acceleration rate, the simulation runs trials with the start amplitude of particles increasing from 0mm at intervals of 0.1mm until the criteria of $\sqrt{2J_z} > 19.3mm^{-1/2}$ is met at some point during an acceleration cycle.

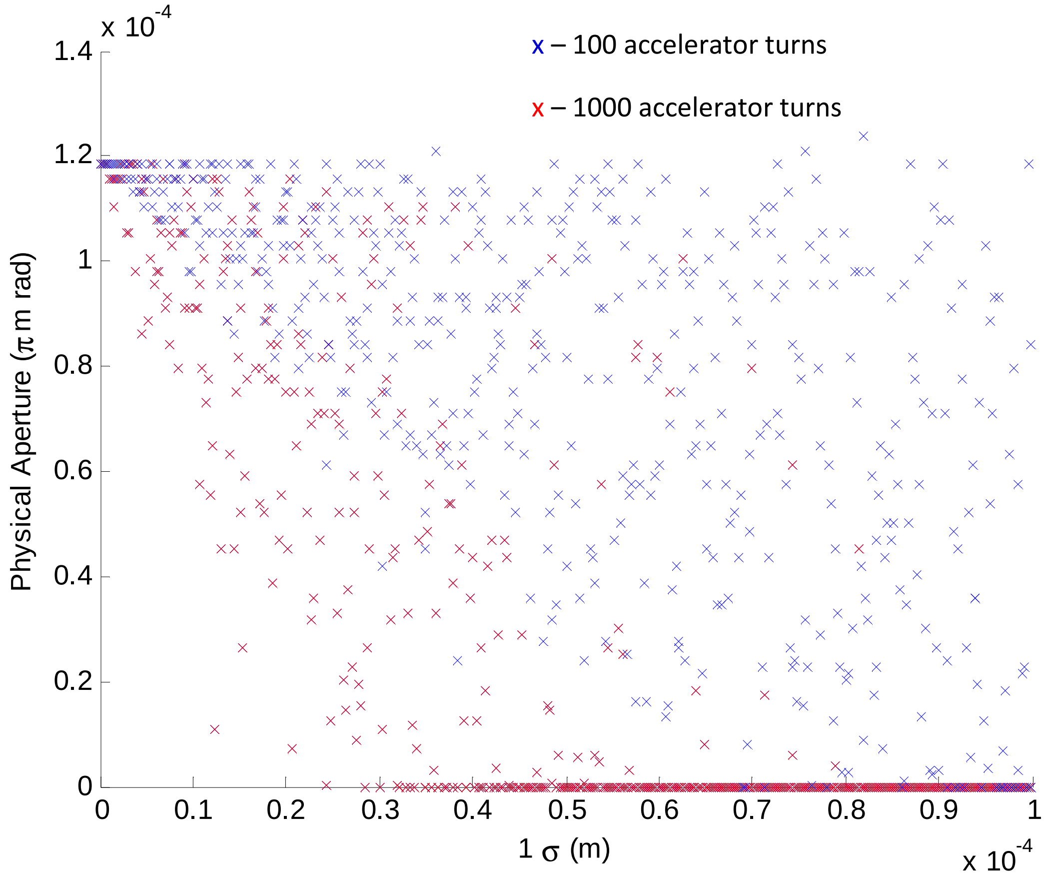

Graph 13: Scatter plot of physical aperture Vs Standard deviation for acceleration through 100 and 1000 turns.

The physical aperture is displayed in units of $\frac{2J_z}{\pi}$ (π m rad).

To give greater clarity when visually interpreting the results displayed in graph 13, averages of the physical aperture over intervals of 15 standard deviations are found and plotted:

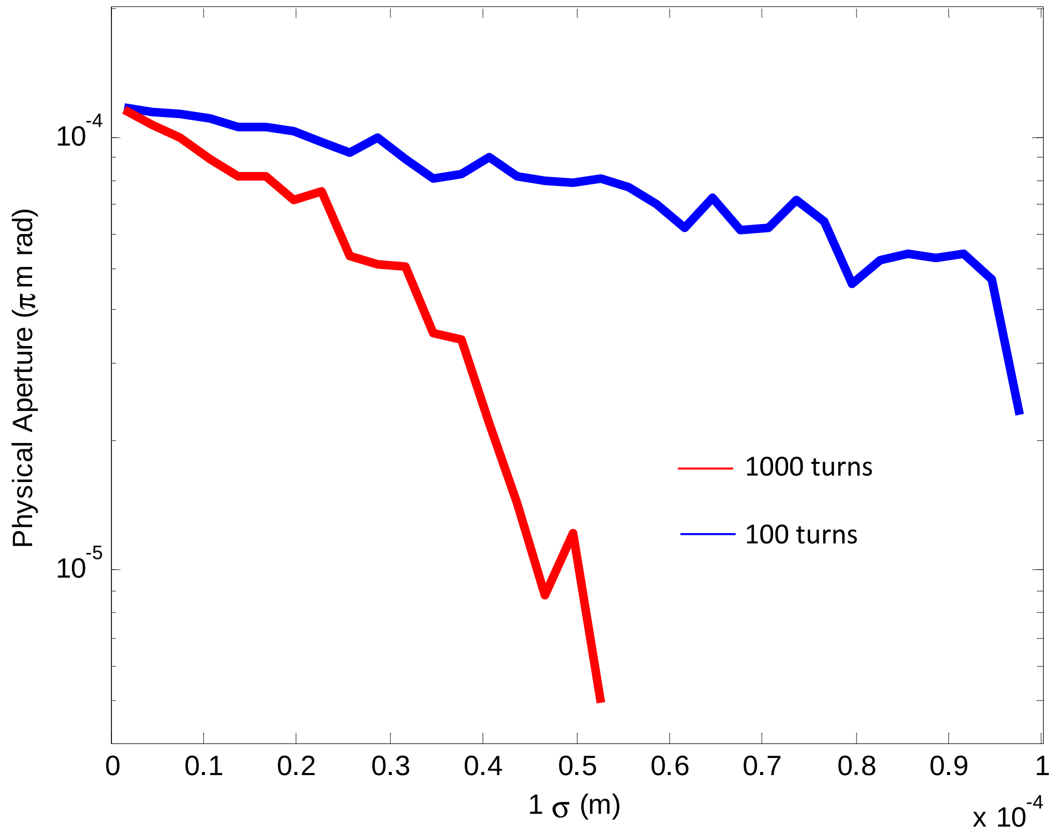

Figure 14: Physical Aperture Vs Standard Deviation (physical aperture averaged at intervals of 15 standard deviation values).

Section IV – Analysis and Conclusion

Analysis and Comparison With a Real Physics Model

Where possible, the parameters of the simulation were set so as to match those used in the model presented by Machida (2008) in the paper *'Resonance Crossing and Dynamic Aperture in Non-scaling Fixed Field Alternating Gradient'*, this was to allow for the evaluation of the approximation that an alternating gradient accelerator may be represented as having a constant gradient when investigating transverse motion behaviour.

Single Particle $\sqrt{2J_z}$ Vs Tune

Plots were produced for the amplitude growth of a single particle as a function of tune (and so energy). The graphs below represent different distributions and standard deviations of alignment errors, and so the meaning of direct comparison is limited. Both plots have been smoothed using Savitzky-Golay filtering (see appendix):

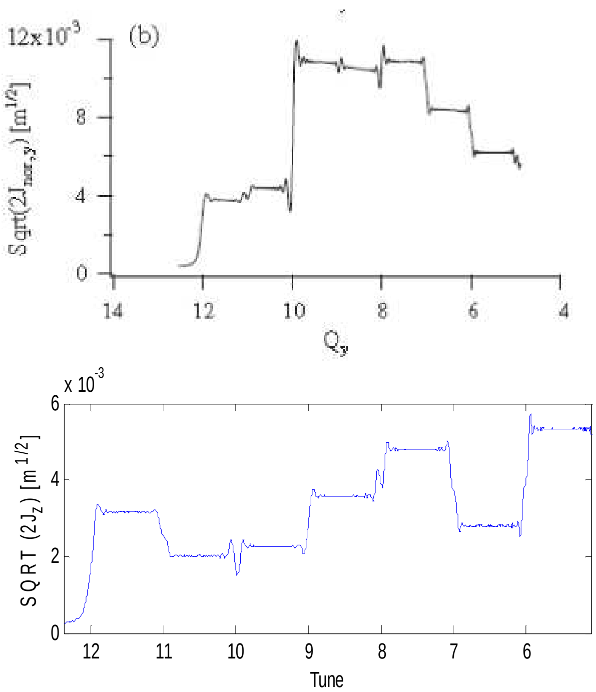

[30]

Graph 14: Amplitude Vs tune for a real physics model (top) and the constant gradient approximation model (bottom), both with acceleration through 1000 turns.

[30] Figure 2 of '*Resonance Crossing and Dynamic Aperture in Non-scaling Fixed Field Alternating Gradient Accelerators'* The axis referred to as 'y' in this plot is equivalent to the axis referred to as 'z' throughout this document.

The amplitude values for the ‘real physics’ model have been normalised with respect to $\beta\gamma$ for this plot of amplitude growth. Also, for the ‘real physics’ model particles were injected at an amplitude which was consistent with the displacement of the phase space origin for a lattice with errors, from the phase space origin without errors, whereas for the constant amplitude model particles were injected with zero amplitude. This finite initial amplitude for the ‘real physics’ model is assumed to be small when compared to the amplitude growth driven by integer tune crossing.

Features consistent with dipole field error driven resonance at integer tune crossing may be seen for both models, these are the sharp changes in amplitude in the vicinity of integer tune values and a relatively small variation in amplitude when the tune is away from integer values.

<u>Effect of the Standard Deviation of Quadrupole Misalignment on Amplitude Growth</u>

By plotting graphs of $\sqrt{2J_z}$ Vs Tune for conditions which may be differentiated only by the standard deviation of the alignment error (i.e. same rate of acceleration, same transverse start amplitude and phase and same error patterns[31]) the following may be obtained:

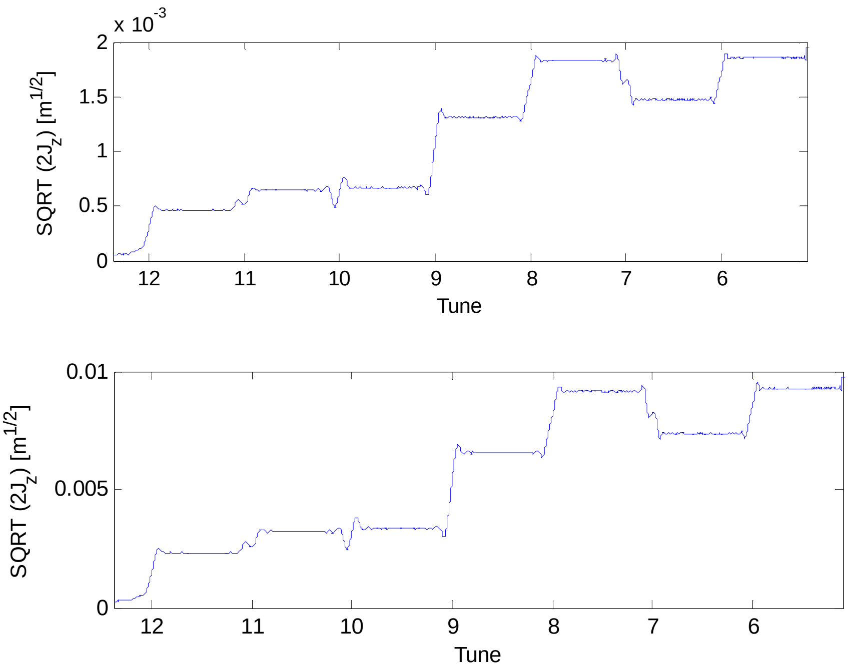

Graph 15: Top quadrupole misalignment distribution with standard deviation of 10 µm, bottom with standard deviation of 50µm. Error patterns identical (i.e. same seed number used for errors).

In essence the plot for errors with standard deviation 50µm is an amplification of the plot obtained for the 10µm distribution. This seems unrealistic, and is potentially as a result of defining the longitudinal velocity as being constant (particularly in the sense of being independent of transverse velocity). In order to gain better understanding of the implications of this approximation, it would be advantageous to develop the model further and give a better representation of a changing longitudinal velocity.

[31] The code for generating quadrupole alignment errors is of the form 'error= µ+ σ*randn(1)'. Altering the standard deviation of the guassian which describes the distribution of quadrupole alignment error essentially scales the errors accordingly.

Effect of the Rate of Acceleration

When making comparisons between the 'real physics' and constant gradient approximated model for plots of the maximum amplitude through acceleration ($\sqrt{2J_{z,max}}$), it is worth noting that Machida seems to suggest that the values of $\sqrt{2J_z}$ for the 'real physics' plot have not been normalised with respect to $\beta\gamma$ (this is contrary to the 'real physics' plot presented in graph 14). The effect of adiabatic damping in this situation will be to give a reduction on the values of $\sqrt{2J_{z,max}}$:

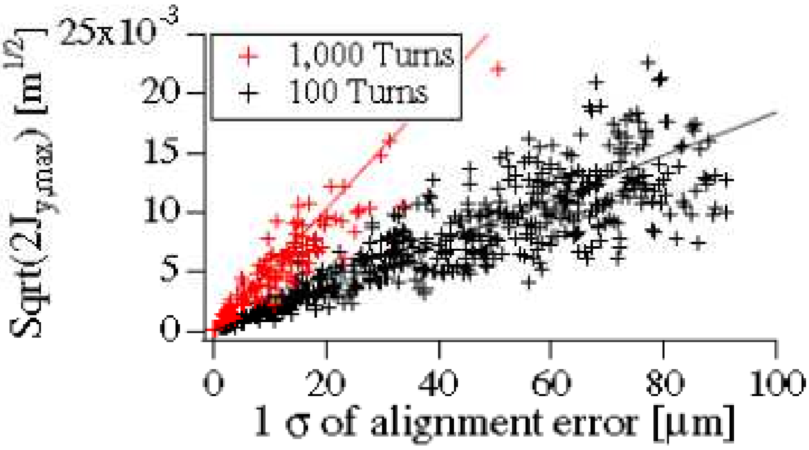

[32]

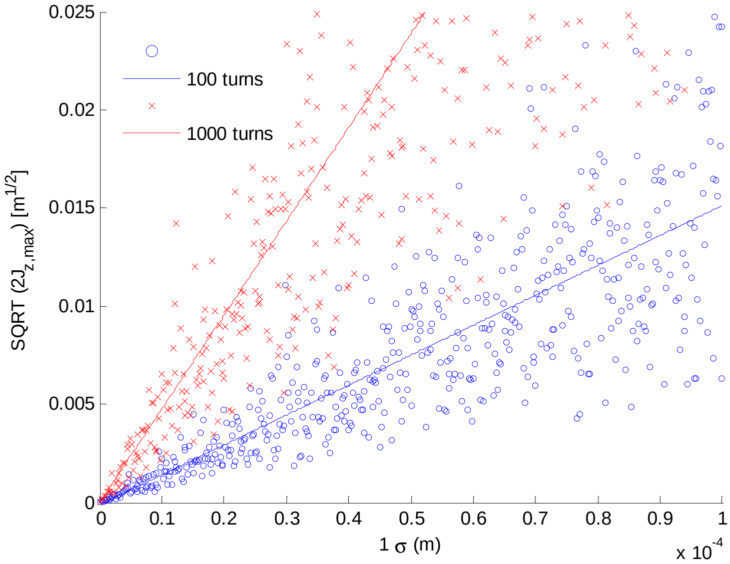

Graph 16: Maximum amplitude Vs standard deviation of quadrupole alignment errors for 'real physics' model (top) and constant gradient approximated model (bottom).

Visual inspection of the plots presented in graph 16 suggests that the rate with which maximum amplitude is found to increase as a function of standard deviation is similar for both models.

[32] Figure 3 of '*Resonance Crossing and Dynamic Aperture in Non-scaling Fixed Field Alternating Gradient Accelerators*'

Comparing graphs of the rate of the maximum amplitude as a function of the standard deviation of quadrupole alignment errors Vs the rate of acceleration confirms this:

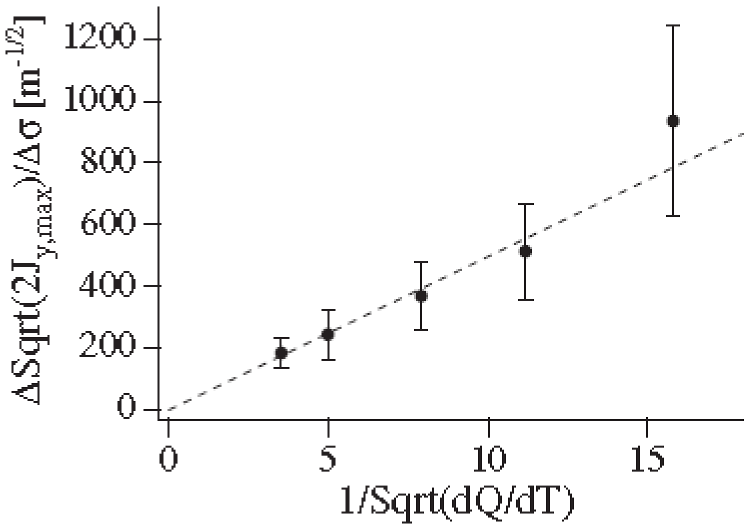

[33]

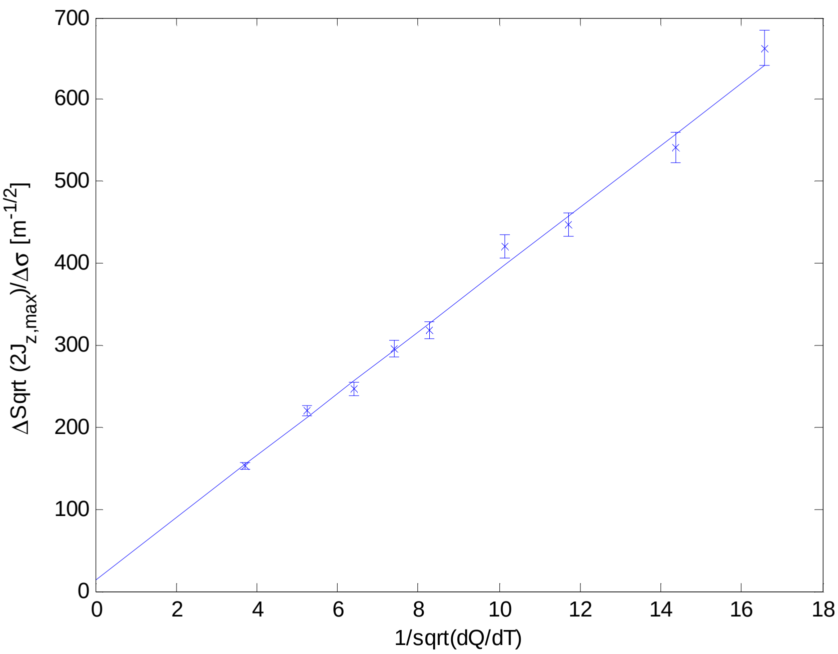

Graph 17: Amplitude growth as a function of acceleration rate for 'real physics' (top) and constant gradient approximation (bottom).

[33] Figure 4 of '*Resonance Crossing and Dynamic Aperture in Non-scaling Fixed Field Alternating Gradient Accelerators*'

The gradients of the line of best fit for graph 17 are:

$$\frac{\Delta\left({}^{\Delta\sqrt{2J_{z,max}}}\!/_{\Delta\sigma} \right)}{\Delta {}^{1}\!\Big/\!\sqrt{{}^{dQ}\!/_{dT}}} = (50 \pm 10\,)m^{-1/2}$$ (20% error) for the 'real physics' model

$$\frac{\Delta\left({}^{\Delta\sqrt{2J_{z,max}}}\!/_{\Delta\sigma} \right)}{\Delta {}^{1}\!\Big/\!\sqrt{{}^{dQ}\!/_{dT}}} = (38 \pm 1\,)m^{-1/2}$$ (3% error) for the constant gradient approximate model

Using a standard consistency check ($|x_1 - x_2| \leq 3\sqrt{{\sigma_1}^2 + {\sigma_2}^2}$) for two measurements $(x \pm \sigma)$ of the same quantity the values are found to be consistent:

$$|50 - 38| \leq 3\sqrt{10^2 + {1_2}^2}$$

However, it may be questionable as to whether the gradients presented are measurements of the same quantity. This is dependent upon the interpretation of the effects of adiabatic damping on the gradient obtained from the plot for the 'real physics' model being correct. Further analysis would be needed in order to confirm the consistency suggested above.

Physical Aperture

Transverse amplitude growth was considered in terms of the apertures of the accelerator, and the minimum initial start amplitude for which a particle would be lost was found for a range of quadrupole error distributions:

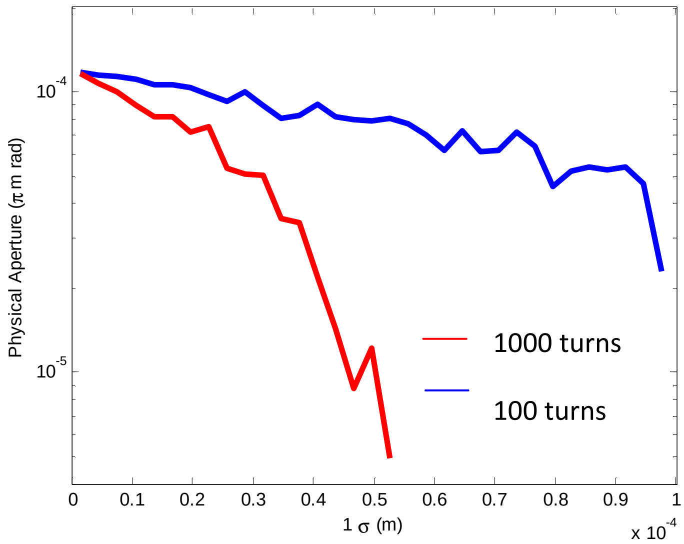

Graph 18: Physical aperture Vs standard deviation of alignment errors as given by the constant gradient approximate model.

For the slower rate of acceleration (through 1000 turns) the initial amplitude for which a particle may be accelerated until the extraction energy falls quickly with increasing quadrupole alignment errors.

For the 'real physics' model a plot of dynamic aperture Vs the standard deviation of alignment error reveals similar behaviour:

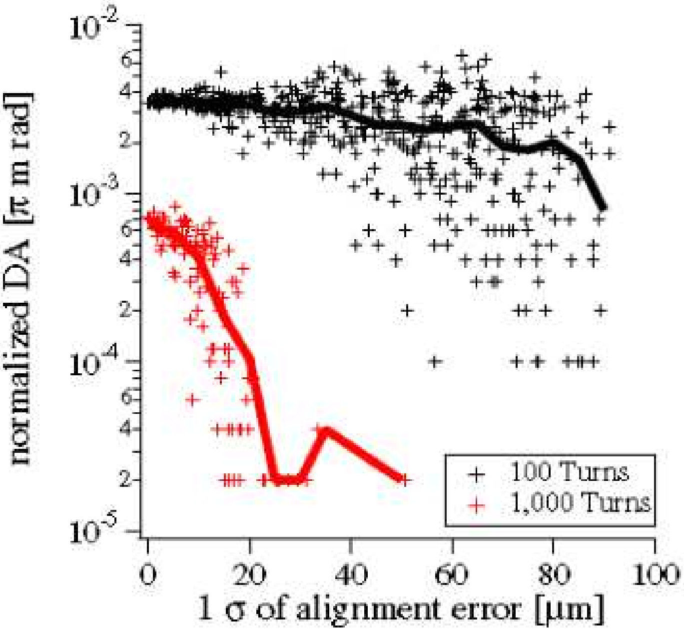

[34]

Graph 19: Dynamic aperture Vs Standard deviation of quadrupole alignment errors as found with the 'real physics' model.

Machida defines the dynamic aperture as being the 'maximum amplitude of survival particles', where a survival particle is one for which the transverse amplitude does not grow to beyond the stable region in transverse phase space. As with the simulation of physical aperture (for the constant gradient approximation), the above plot is obtained by locating the maximum[35] initial amplitude for which a certain value of amplitude is not met throughout acceleration.

What is not immediately clear, is the reason behind the difference in dynamic aperture for acceleration through 100 turns and 1000 turns when there are no quadrupole alignment errors present (for the physical aperture plot the lines for both rates of acceleration converge with no alignment errors).

[34] Figure 5 of '*Resonance Crossing and Dynamic Aperture in Non-scaling Fixed Field Alternating Gradient Accelerators*'

[35] For the relative size of interval the maximum initial amplitude for which a condition is not met may be approximated to the minimum initial amplitude for which a condition is met.

Conclusion

It is difficult to give an evaluation of the quantitive agreement between models without understanding the exact parameters of both; however these initial findings suggest that there is consistency.

The approximation of alternating gradient focusing to constant gradient focusing was found to be effective in demonstrating the fundamental behaviour of transverse amplitude growth when resonance at integer tune values is driven by dipole field errors; With the ability of a linear NS-FFAG to accelerate a particle to an extraction energy being dependent upon the rate of acceleration and the magnitude of the quadrupole alignment errors within the accelerator.

Looking at figure 7, it can be seen that the relationship between the phase of the transverse motion and the location of quadrupoles is dependent upon the properties of the lattice. This is something that has not been accounted for a within the constant gradient approximated model, and the effects of which, I feel, are worthy of further investigation.

Neither model explores the effect of resonances as a result of tune variation within EMMA fully, with only dipole field errors considered. Higher order errors, such as quadrupole field errors, will introduce resonances at non integer tune values (when the tune value is a simple fraction, e.g. half integer)[36]. A more complete model could investigate these effects of these too.

In terms of the suitability of the NS-FFAG for proton therapy applications, the attraction to a relatively low cost combination of the intensity of a cyclotron and the flexibility of a synchrotron is clear. For the linear NS-FFAG studied, the nature of amplitude growth with relation to the standard deviation of quadrupole alignment errors and rate acceleration may mean that a non-linear NS-FFAG lattice design[37] must be considered for proton acceleration(Machida(2008)).

[36] Brandt,D (2004) *Accelerator Basics* presentation. Available at http://cas.web.cern.ch/CAS/Warrington/PDF/Brandt5.pdf

[37] Which may limit the tune excursion in order to exclude integer tune values.

SECTION V – APPENDIX

Summary of the article:

Resonance Crossing and Dynamic Aperture in

Non-scaling Fixed Field Alternating Gradient Accelerators[38]

The article, written by Shinji Machida, describes an investigation into the effect of quadruple alignment errors and the rate at which particle acceleration occurs upon the amplitude of a particle for a linear nsFFAG. Within the abstract for the article Machida reports that for a typical error of 10μm rms, that there is 'practically no dynamic aperture' for slow acceleration (through 1000 turns).

The following offers a brief summarisation of the article, with the aim of presenting Machida's simulation results (which shall act as a comparison for the output of the simulation being developed as part of the Phys498 project).

I. Introduction

Machida begins by introducing the concept of accelerating muons (to energies of 20 or 50 GeV) through the use of a scaling (s) FFAG. The betatron tune for a sFFAG remains constant for both planes through acceleration, however, for a nsFFAG this is not the case as tune varies with inverse proportionality to energy (see graph below). As a particle is accelerated the tune crosses through integer values, and it is in these regions that kicks from misaligned magnets lead to dramatic growth in particle amplitude (and the eventual loss of the particle to the accelerator wall).

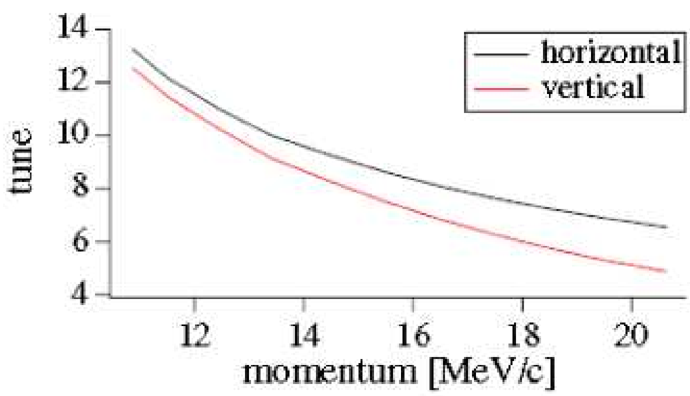

Graph 20: Tune Vs Momentum

The muon lifetime (2.2μs) means that rapid acceleration must be utilised in order to reach the energies quoted above (with acceleration occurring over 10 to 20 turns), in this instance there is no destructive build up in amplitude as a result of traversing integer tunes. For other anticipated applications of nsFFAG's, such as for particle therapy, priority shifts from rapid acceleration (proton

[38] Machida, S. (2008) *Resonance Crossing and Dynamic Aperture in Non-scaling Fixed Field Alternating Gradient Accelerators*

lifetime many orders of magnitude higher than that of the muon) to reducing costs (accelerators with lower rf voltages).

It is for these slower rates of acceleration that resonance crossing becomes problematic, and, for this reason, Machida raises the importance of determining the feasibility of such acceleration regimes.

II. Simulation Setup

A. Accelerator Model

The EMMA lattice is used as a basis for simulation.

Several assumptions were made:

- Particle energy increased by a constant amount at each cell (to represent acceleration).
    1. *Discounts the effects of longitudinal and transverse coupling:*
       For the EMMA lattice, the time take for one revolution for a particle is dependent upon the transverse amplitude (as larger amplitude particles follow a larger path). This difference in revolution time leads to energy spread in a bunch, and for a particle with amplitude beyond a critical magnitude, entering the deceleration phase of the rf will lead to the particles loss.
    2. *Leads to a reduction in processing time for the simulation.*
    3. *Acceleration occurs at each cell rather than at periods consistent with the location of the 19 rf cavities so as not to create additional symmetries within the lattice.*
- Simulation injection and extraction energies of 10.75 and 20.75 MeV (rather than EMMA values of 10.50 and 20.50 MeV).
  Acceleration begins with horizontal and vertical tune values away from integer quantities and results in lower initial orbit distortion.
- Transverse amplitude growth is stimulated by quadrupole misalignment. The focussing and defocusing quadrupoles of a cell, which are located on the same table, are assumed to be misaligned in the same direction and by the same magnitude. Rotational and longitudinal misalignments of quadrupoles are neglected.

B. Particle Amplitude

The value of J_y is the action for the particle in yy' plane, values will exhibit adiabatic damping.

$$2J_y = \frac{y^2 + \left(\alpha_y + \beta_y y'\right)^2}{\beta_y}$$

III. Simulation Results

A. Single Particle Behaviour

Machida presents the development of normalized (with respect to relativistic βγ) vertical amplitude with decreasing tune (i.e. increasing particle energy). Vertical motion is selected due to its similarity to horizontal motion and the smaller vertical aperture.

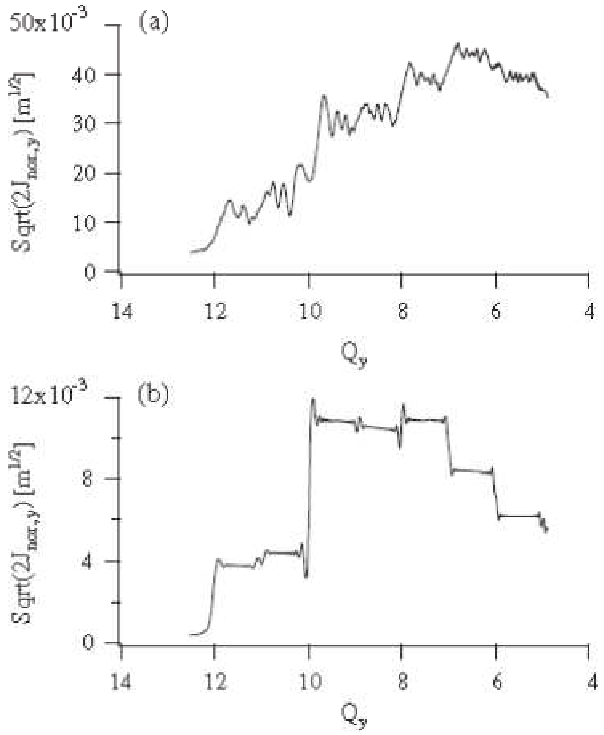

Graph 21: Normalised amplitude Vs tune for (a) 100 turns and (b) 1000 turns. Magnitude of misalignment in (a) higher than that of (b) hence larger amplitudes for (a)

Graphs 2.a and b. demonstrate how amplitude growth is related to the rate of acceleration; with the slower rate of acceleration (through 1000 turns) showing dramatic amplitude changes at integer tune values.

The rate at which the maximum transverse amplitude increases with the standard deviation of the quadrupole misalignment error is shown to be dependent upon the rate of acceleration:

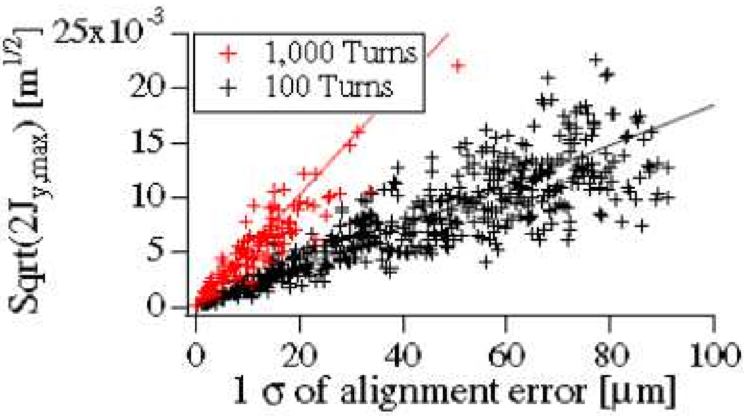

Graph 22: Maximum particle amplitude (through acceleration) Vs the standard deviation of the alignment errors for acceleration through 100 and 1000 turns.

The growth of maximum amplitude with respect to acceleration rate:

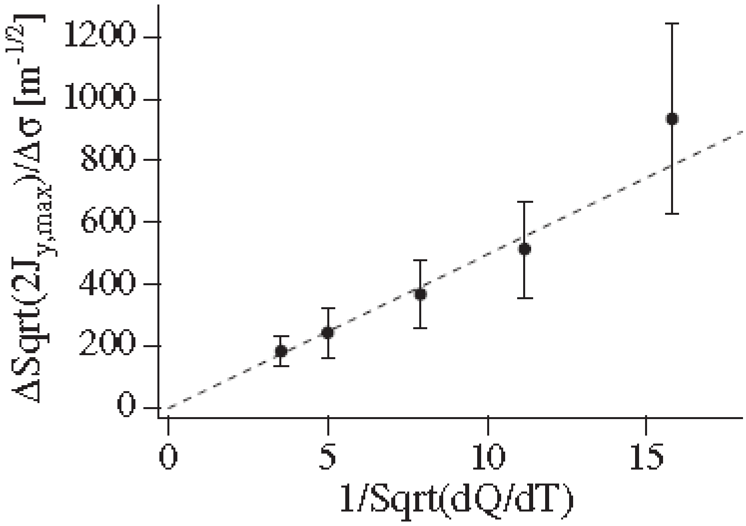

Graph 23: (Figure 4 form Machida's paper) Amplitude growth as a function of acceleration rate.

According to Machida, graph 20 has a gradient of $50m^{-1/2}$, based upon the same method of error calculation as utilised for the constant gradient approximate model the value with uncertainty can be taken as $(50\pm10)m^{-1/2}$.

B. Dynamic Aperture

Machida explains how the growth of amplitude may result in a particle not being accelerated to the final energy and defines the dynamic aperture as being the maximum initial amplitude of 'survival' particles. Here a survival particle is classed as one which is not accelerated to outside the region of stable phase space.

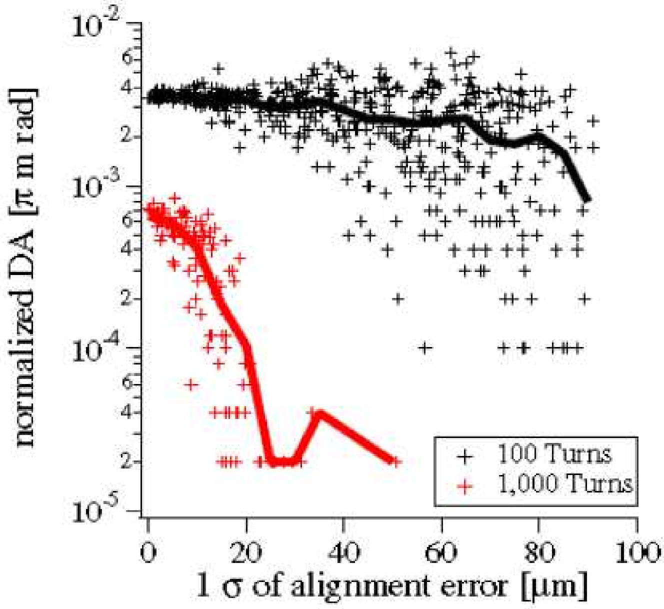

Graph 24: (Figure 5 from Machida's paper) Dynamic aperture Vs standard deviation of alignment error, with solid lines showing average of nearby points.

Machida notes that there is no dynamic aperture when quadrupoles have alignment errors of more than 15μm when acceleration occurs over 1000 turns.

Testing of Basic Model

Zero amplitude does not grow without perturbation:

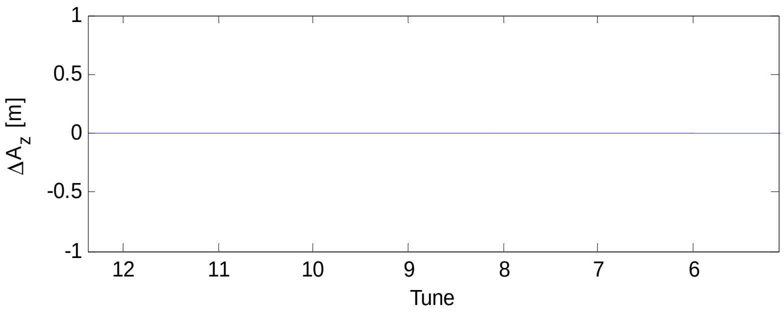

Graph 25:Start amplitude 0mm and standard deviation of alignment error magnitudes of 0m.

Amplitude (mm) increases as a function of energy regardless without the effects of dipole field errors. Model equivalent to simple harmonic motion for a spring with constantly weakening spring constant k:

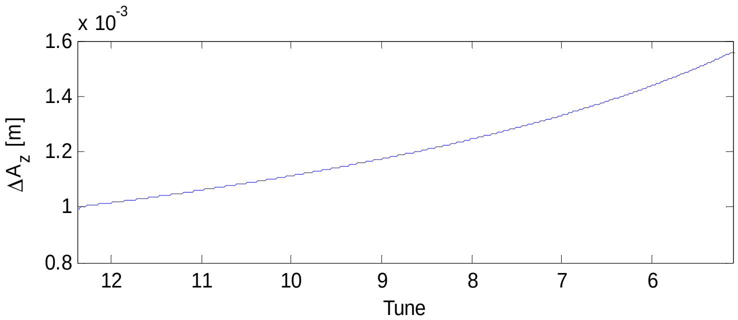

Graph 26: Start amplitude of 1mm and standard deviation of alignment error magnitudes of 0m.

Amplitude in terms of $\sqrt{2J}$ is constant with increases energy.

The effect of a transverse velocity kick upon an oscillator can be to increase the transverse amplitude:

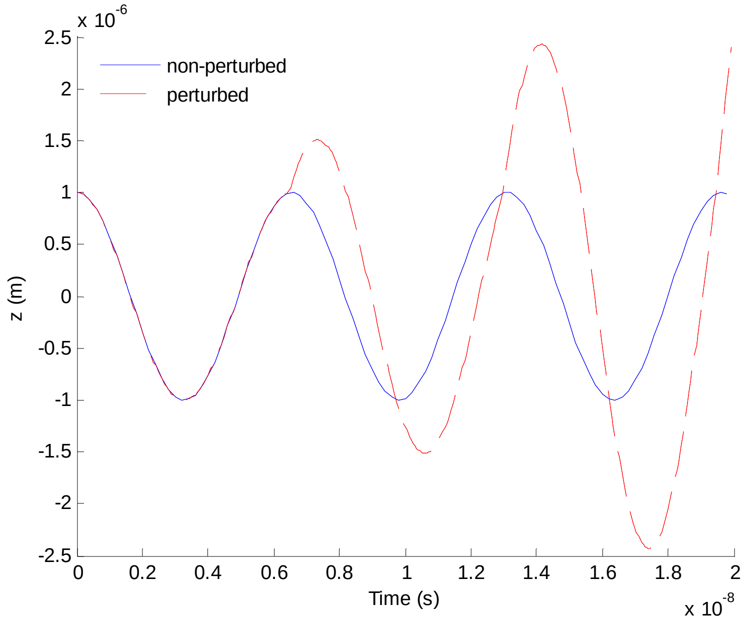

Graph 27: The effect of a periodic perturbing influence (at intervals of 65ns) on a 960 Mrads^{-1} oscillator.

Presentation of Results for $\sqrt{2J_z}$ Vs Tune

Savitzky-Golay filtering is a method that smoothes noisy data whilst preserving features such as minima and maxima. The filter functions by fitting a polynomial of the nthdegree at intervals of x (where n and x are variable) to data.

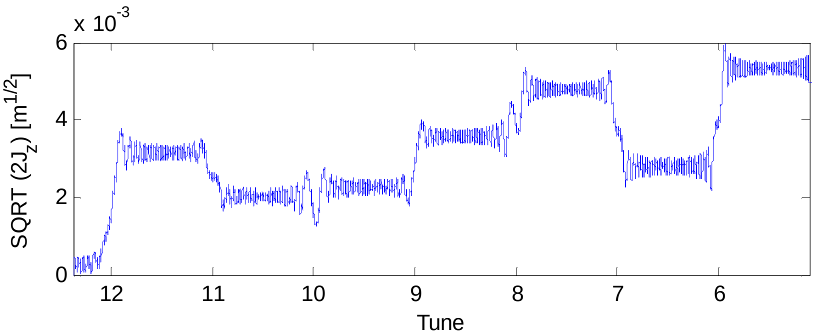

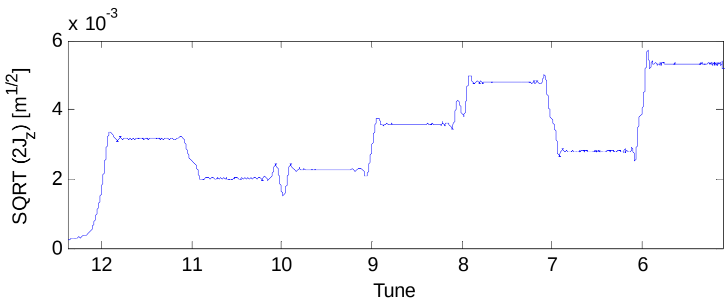

Graph 28: Top-Without Savitzky-Golay filter. Bottom-With Savitzky-Golay Filter

EMMA CELL PARAMETERS

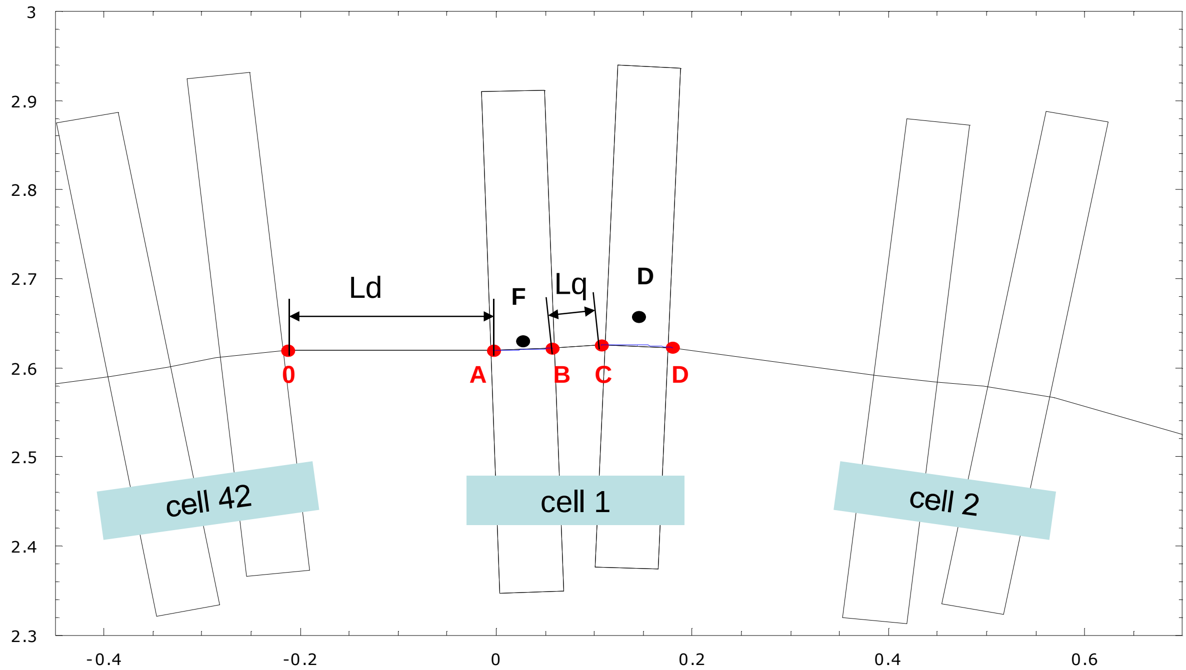

[39]

Figure 15: EMMA cell layout.

F0D0 properties:

Number of cells in EMMA	42
Long drift length	0.210m
Short drift length	0.055m
Defocusing quadrupole Length	0.071m
Defocusing quadrupole gradient	-4.892Tm^{-1}
Focussing quadrupole length	0.058m
Focussing quadrupole gradient	6.650Tm^{-1}
Total length	16.573m

Table 2: Some of the EMMA geometrical information relevant to this project.[40]

Quadrupole Aperture data:

	Defocusing	Focusing
Separation	50mm	
Yoke lengths	65mm	55mm
Inscribed radii	51mm	36mm
Aperture (h)	26.2mm	42.3mm
Aperture (v)	23.4mm	17.8mm
Max. field (T)	0.44	0.48

Table 3:focusing and defocusing quadrupole parameters.[41]

[39] Conform (2007) *EMMA cell layout*. Available at http://www.astec.ac.uk/emmafiles/magnets/EMMAcelllayout.ppt
[40] Conform (2007) *EMMA geometry*. Available at http://www.astec.ac.uk/emmafiles/magnets/EMMA Geometry.xls

Betatron tune:

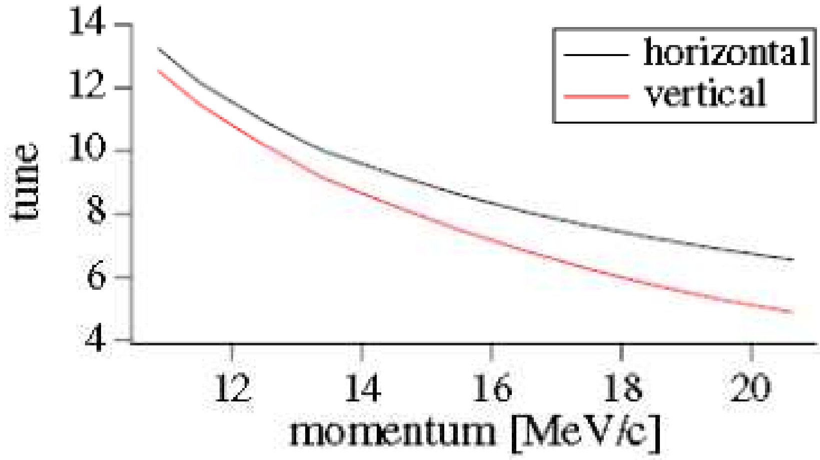

Given that the betatron tune is a function of the lattice, the relationship between betatron tune and energy was defined in the simulation by a 2nd order polynomial fit to the data presented by S.Machida.

$Q_z = 0.0549E^2 - 3.4572E + 32.4479$

$Q_z = 0.0621E^2 - 2.5827E + 33.7552$

Where E is the energy.

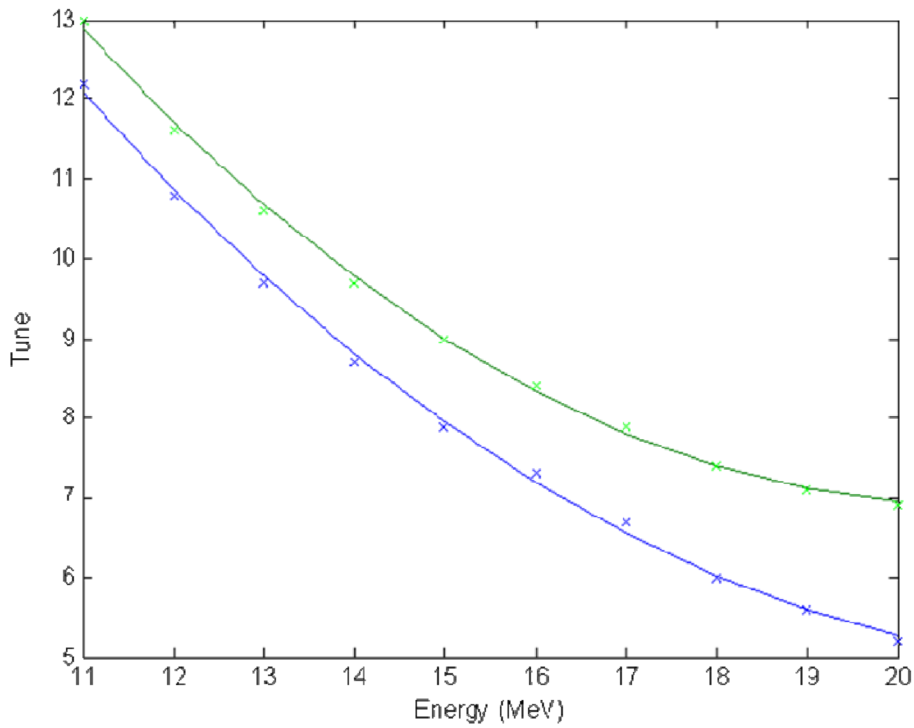

Graph 29: Plot of vertical (blue) and horizontal (green) tune as a function of energy. As given by polynomial fit.

[41] Edgecock,R. (2007) *EMMA – THE WORLD'S FIRST NON-SCALING FFAG*

MATLAB CODE

1. Matlab program (ex3multikickcurvytune.m) for producing results in the form:

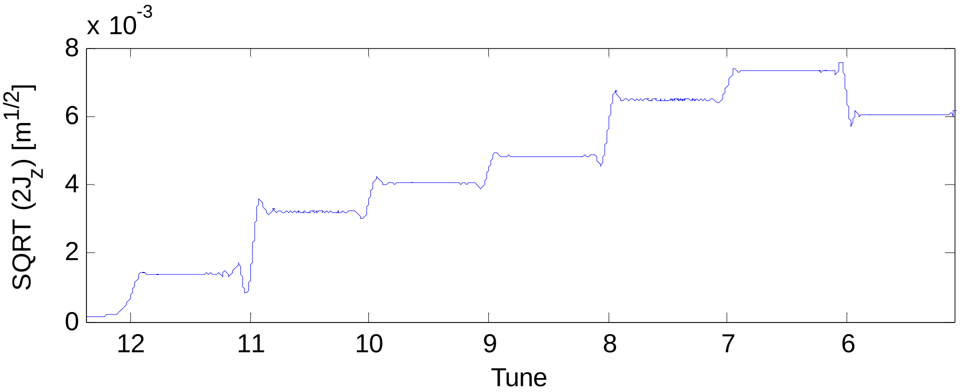

Main Program:

```
clear all

% to simulate the effect of 84 kicks per revolution

% on an electron in EMMA

% assuming uniform focusing strength
%------------------------------------------------
%Constants throughout simulation
global Q qe LightSpeed
N0 = 1000;     % no. of turns
CT = 42*N0;    %number of cells traversed
L = 16.57;   % (m) Circumference

%Quadrupole details ( Column 1 is focussing and 2 is defocussing,
%row 1 is field gradient and 2 is quadrupole length)
Q = [6.7,        -4.9
     58.782e-3, 75.699e-3];

qe = 1.602e-19; %electron charge
LightSpeed = 2.998e8;   %  (m/s)  speed of light
T0 = L/LightSpeed; %time taken for one revolution
TDF = 0.274571/LightSpeed; %time taken to travel from defocussing to
focussing quad centre
TFD = 0.120023/LightSpeed; %time taken to travel from focussing to
defocussing quad centre
%------------------------------------------------
% set matrices of before and after position and velocity
A1 = zeros (1, CT);
x1 = zeros(1, CT);  %
v1 = zeros(1, CT);  % x1(m)displacement & v1(m/s) velocity after one cell
beta1 = zeros(1, CT);
tunegraph = zeros(1,CT);
%------------------------------------------------
%Acceleration parameters
%Energy range
Estart = 10.75; %Injection energy MeV
Estop = 20.75; %Extraction energy MeV
deltaE = (Estop - Estart)/CT; %energy increase per cell
```

```
%-------------------------------------------------
%distribution of misalignments and associated forces
mu=0; %mean
sigma=20e-6; %standard deviation
seed = 774; %seed for repeating results with pseudo random number
F = gauerr(mu, sigma, seed);
%--------------------------------------------------
% Particle Start parameters
tunemin = (0.0549*Estop^2) - (2.4572*Estop) + 32.4479;
tunemax = (0.0549*Estart^2) - (2.4572*Estart) + 32.4479;
beta1(1) = L/(2*pi*tunemax); % beta start value
freq = tunemax / T0;
wb = 2*pi*freq;
%---------------------------------
A1(1)=0e-3;     % (m) start amplitude
x1(1) = 1*A1(1);      % (m) start displacement
v1(1) = sqrt(wb^2*(A1(1)^2-x1(1)^2));   % (m/s) start velocity
%---------------------------------
%counting
c=1; %cell number

for c1 = 1:(CT-1),
  energy = Estart + c1*deltaE; %accelerartion
  tune = (0.0549*energy^2) - (2.4572*energy) + 32.4479;
  tunegraph (c1) = tune;
  freq = tune / T0;
  wb = 2*pi*freq;

  dvF = (F(c,3) * LightSpeed * Q(2,1))/(energy*1e6*qe); %transverse
  velocity kick at focussing quad
  dvD = (F(c,4) * LightSpeed * Q(2,2))/(energy*1e6*qe); %transverse
  velocity kick at defocussing quad

  vector1 = [x1(c1)
            v1(c1)];

  M = M1(wb, TDF);
  vector2 = M * vector1;   %travel from previous defocussing quad to
subsequent focussing quad
  vector2(2)=vector2(2) + dvF; %adds focussing quad kick to vector

  M = M1(wb, TFD);
  vector2 = M * vector2;  %travel from previous focussing quad to
subsequent defocussing quad
  vector2(2)=vector2(2) + dvD; %adds defocussing quad kick to vector

  x1(c1+1) = vector2(1);
  v1(c1+1) = vector2(2);
  A1(c1+1) = sqrt(x1(c1+1)^2 + (v1(c1+1)^2 / wb^2));
  beta1(c1+1) = L/(2*pi*tune);
  A1(c1+1)= A1(c1+1)/sqrt(beta1(c1+1));
  c = c+1;
  if c>42 %42 cells in EMMA
      c=1;
  end
end

%-----------------------------------------
```

```
turn = 0:(N0-1);     %  turn number for graph
SA1 = sgolayfilt(A1,1,301); %Savitzky-Golay filter
subplot (2,1,1)
plot(tunegraph, SA1)     %plots processed data
set(gca,'XDir','reverse','XLim',[tunemin tunemax])
xlabel('Tune')
ylabel('SQRT (2J_{z}) [m^{1/2}]')
subplot (2,1,2)
plot(tunegraph, A1)        %plots raw data
xlabel('Tune')
ylabel('SQRT (2J_z) [m^{1/2}]')
```

<u>Random Cell Alignment Generator (gauerr.m):</u>

```
%function to produce an array of errors
function F = gauerr(mu, sigma, seed)
global Q qe LightSpeed
err = zeros(42,1); %Quad error matrix
F = zeros(42,4); % Quad error force matrix
randn('seed',seed);
rand('seed',seed+100);
for x=1:42
    z = 2*sigma +1;
    while z >(2*sigma)  %for as long as the error magnitude is larger than
2*sigma cut off
    errmag=mu+ sigma.*randn(1);
    z = sqrt(err(x)^2);
    end
    theta = rand * 2*pi;
    err(x,1) = errmag * cos(theta);
    err(x,2) = errmag * sin (theta); % gives x and y components of
alignment error
    F(x,1)=qe*LightSpeed*Q(1,1) *err(x,1); %horizontal focussing force
    F(x,2)=qe*LightSpeed*Q(1,2) *err(x,1); % horizontal defocussing force
    F(x,3)=qe*LightSpeed*(-Q(1,1)) *err(x,2); %vertical focussing force
    F(x,4)=qe*LightSpeed*(-Q(1,2)) *err(x,2); % vertical defocussing force
end
end
```

<u>SHM Transfer Matrix (M1.m):</u>

```
%SHM Matrix function
function transfer = M1(wb, T)
transfer = [cos(wb*T)   1/wb*sin(wb*T)
          -wb*sin(wb*T)  cos(wb*T)];
end
```

2. Matlab program (ex4.m) for producing results in the form of:

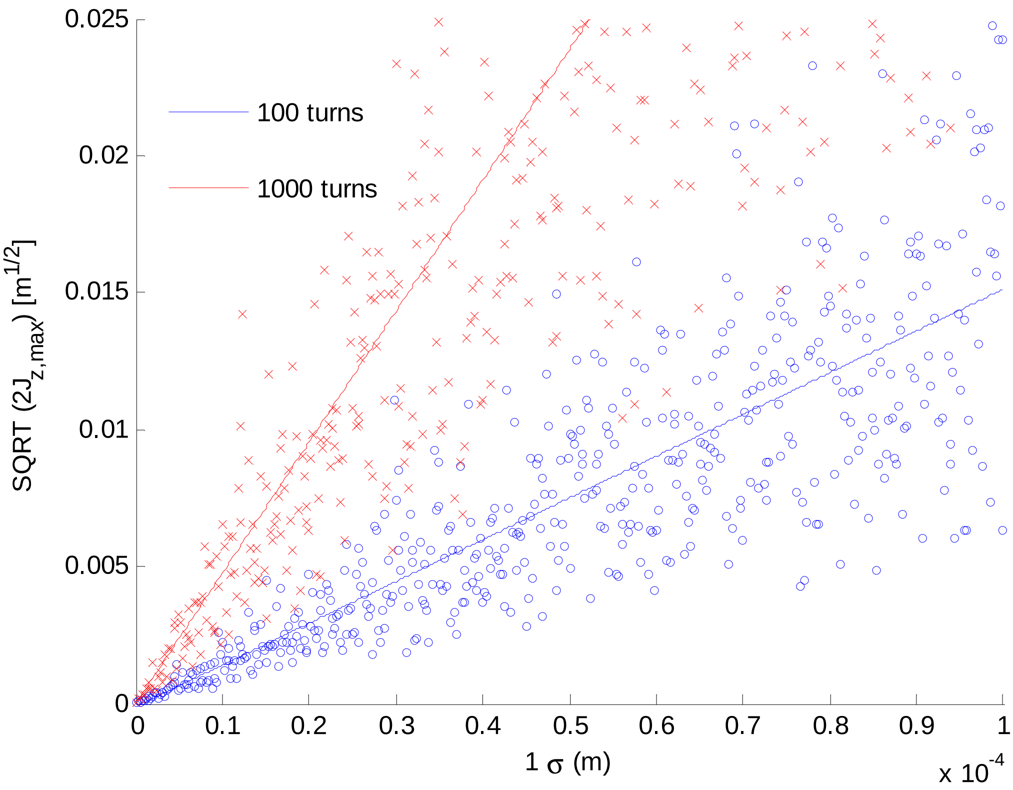

-

<u>Main Program:</u>

```
Clear all

% to simulate the effect of 84 kicks per revolution
% on an electron in EMMA assuming uniform focusing strength
% to produce graphs of maximum amplitude through N turns with relation to
% increasing sigma values for the distribution of quadrupole alignment
% errors (500 unique error patterns).
%-------------------------------------------------

N0 = [100, 1000];     % no. of turns
n=numel(N0);  %number of elements in the array N0
global Amax
Amax = zeros(500,n);
for turnset = 1:n
    N = N0(turnset);
    ex4Nturns(turnset, N);
end

%-----------------------------------------
%Graphing
sigma = [1:500]' .*((1e-6)/5); %Sigma from 0.2 to 100 micrometers
for b=1:n
  if b==1
    scatter(sigma, Amax(1:500,b), 10,'b')
    axis([0 1e-4 0 0.025])
    xlabel('1 \sigma (m)')
```

```
    ylabel('SQRT (2J_{z,max}) [m^{1/2}]')
    hold on
    p = polyfit (sigma, Amax(1:500,b),1); %fits line of best fit to data
    lobf =  p(1) .*sigma +p(2);
    plot (sigma, lobf) %plots line of best fit to data
  end
  if b==2
    scatter(sigma, Amax(1:500,b), 20,'rx')
    p = polyfit (sigma, Amax(1:500,b),1); %fits line of best fit to data
    lobf =  p(1) .*sigma +p(2);
    plot (sigma, lobf,'Color','red') %plots line of best fit to data
  end
 end
    hold off
```

Program for Calculating the Maximum Amplitude Given a Rate of Acceleration and Standard Deviation of Alignment Errors:

```
function ex4Nturns(turnset, N)
global Q qe LightSpeed Amax
CT = 42*N;   %number of cells traversed
L = 16.57;   % (m) Circumference
%Quadrupole details ( Column 1 is focussing and 2 is defocussing,
%row 1 is field gradient and 2 is lattice length)
lqf = 58.782e-3; %length of horizontally focusing quad
lqd = 75.699e-3; %length of horizontally defocusing quad
Q = [6.7, -4.9
     lqf, lqd];

qe = 1.602e-19; %electron charge
LightSpeed = 2.998e8;   %  (m/s)  speed of light
%Assumes straight paths!
T0 = L/LightSpeed; %time taken for one revolution
TDF = 0.274571/LightSpeed; %time taken to travel from defocussing to
focussing quad
TFD = 0.120023/LightSpeed; %time taken to travel from focussing to
defocussing quad
%-------------------------------------------------
% set matrices of before (1) and after (2) position and velocity
x1 = zeros(1, CT);  %
v1 = zeros(1, CT);  % x1(m)displacement & v1(m/s) velocity after one cell
A1 = zeros(1, CT);
beta1 = zeros(1, CT);
tunegraph = zeros(1,CT);
%-------------------------------------------------
%Acceleration parameters
%Energy range
Estart = 10.75; %Injection energy MeV
Estop = 20.75; %Extraction energy MeV
deltaE = (Estop - Estart)/CT; %energy increase per cell

for nxsigmamin = 1:500
%-------------------------------------------------
%distribution of misalignments and associated forces
mu=0; %mean
sigma= nxsigmamin*(1E-6)/5; %standard deviation
seed = nxsigmamin^2; %to provide repeatable values for testing
F = gauerr(mu, sigma, seed);
```

```
%-------------------------------------------------
% Particle Start parameters
tunemax = (0.0549*Estart^2) - (2.4572*Estart) + 32.4479;
freq = tunemax / T0;
wb = 2*pi*freq;
beta1(1) = L/(2*pi*tunemax); % beta start value
x1(1) = 0;   % (m) start displacement
v1(1) = 0;    % (m/s) start velocity
A1(1) = sqrt(x1(1)^2 + v1(1)^2 / wb^2);
%counting
c=1;
for c1 = 1:(CT-1),
  energy = Estart + c1*deltaE;
  tune = (0.0549*energy^2) - (2.4572*energy) + 32.4479;
  tunegraph (c1) = tune;
  freq = tune / T0;
  wb = 2*pi*freq;

  dvF = (F(c,3) * LightSpeed * Q(2,1))/(energy*1e6*qe); %transverse
velocity kick at focussing quad
  dvD = (F(c,4) * LightSpeed * Q(2,2))/(energy*1e6*qe); %transverse
velocity kick at defocussing quad

  vector1 = [x1(c1)
            v1(c1)];

  M = M1(wb, TDF);
  vector2 = M * vector1;   %travel from previous defocussing quad to
following focussing quad
  vector2(2)=vector2(2) + dvF; %adds kick from horizontally focussing quad
to vector
  M = M1(wb, TFD);
  vector2 = M * vector2;  %travel from previous focussing quad to following
defocussing quad
  vector2(2)=vector2(2) + dvD; %adds kick from horizontally defocussing
quad to vector

  x1(c1+1) = vector2(1);
  v1(c1+1) = vector2(2);

  beta1(c1+1) = L/(2*pi*tune);
  A1(c1+1) = sqrt((x1(c1+1))^2 + (v1((c1+1))^2 / wb^2));
  c = c+1;
  if c>42
      c=1;
  end
end
% Maximum amplitude for nxsigmamin errors over N turns
A1 = A1 ./ sqrt(beta1);
Amax(nxsigmamin, turnset) = max(A1);
end
end
```

Random Cell Alignment Generator (gauerr.m):

Refer to gauerr.m in the first programming section.

SHM Transfer Matrix (M1.m):

Refer to M1.m in first programming section.

3. Matlab program (ex5.m) producing a graph of the rate of change of maximum amplitude with respect to sigma Vs the rate of acceleration:

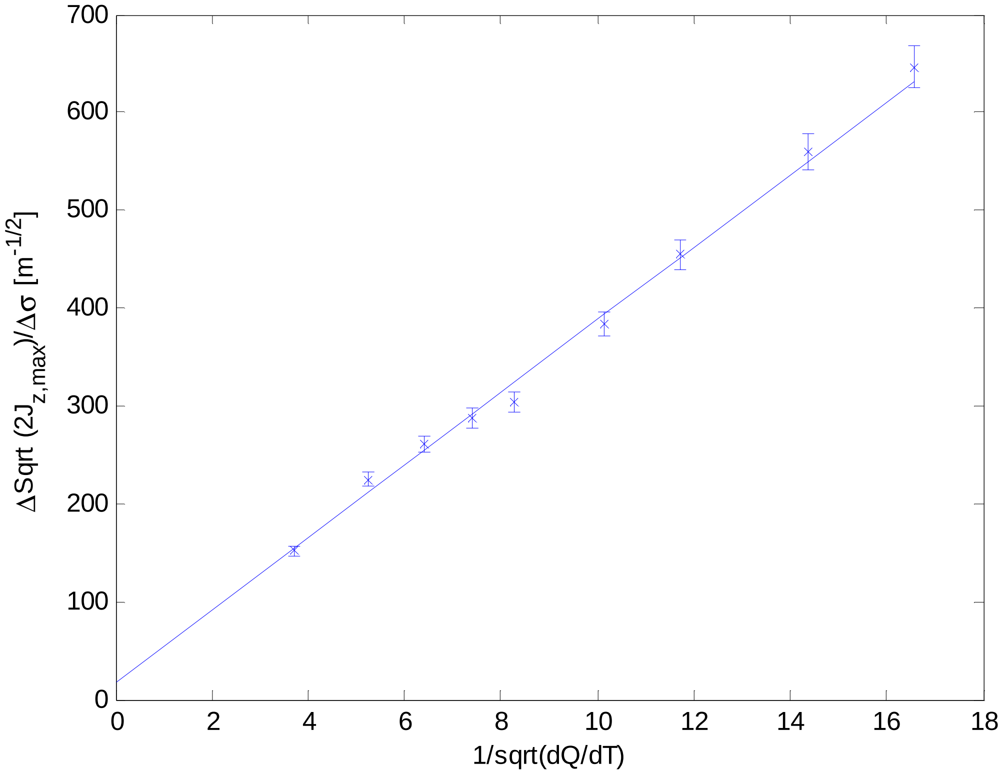

Main Program:

```
clear all

% to simulate the effect of 84 kicks per revolution

% on an electron in EMMA

% assuming uniform focusing strength

% to produce graphs of the rate of change of maximum amplitude with respect

% to sigma Vs the rate of acceleration.
%-------------------------------------------------

N0 = [100, 200,300, 400, 500,750, 1000,1500, 2000];    % no. of turns
n=numel(N0);  %number of elements in the array N0
global Amax GradTune
Amax = zeros(500,n);
GradTune = zeros(1,n);
for turnset = 1:n
    N = N0(turnset);
    ex5Nturns(turnset, N);
    (turnset/n)*100
end

%-----------------------------------------

sigma = [1:500]' .*((1e-6)/5);
```

```
p=zeros(1,n);
RMSD = zeros(1,n);
%fits line of best fit to data for each rate of acceleration and calculates
%an error on the gradient of this line based upon the distribution of
%points around it.
for b=1:n
    fit4Nturns = polyfit (sigma, Amax(1:500,b),1);
    p(1,b)=fit4Nturns(1);
    trend = fit4Nturns(1).*sigma + fit4Nturns(2);
    Err1 = 0;
    for errc=1:500
    Err1 = Err1 + (Amax(errc,b) - trend(errc,1))^2;
    end
    RMSD(1,b)= sqrt(Err1/498);
    sumsigsq = sum(sigma.^2);
    sqsumsig = sum(sigma)^2;
    errgrad(1,b)=RMSD(1,b)* sqrt(500/((500*sumsigsq)-sqsumsig));
end
d = 1./sqrt(GradTune);

%--------------------------------------------
%Least square fit
Nu = numel(d);
meand = sum(d)/N;
meandsq= sum(d.^2)/N;
%---------------------------------------------
%Gradient and constant for line in the form y=mx+c
S = sum(1./(errgrad.^2));
Sxy = sum ((d.*p)./(errgrad.^2));
Sx = sum (d./(errgrad.^2));
Sy = sum (p./(errgrad.^2));
Sxx = sum ((d.^2)./(errgrad.^2));
delta = (S*Sxx)-(Sx^2);
m = ((S*Sxy)-(Sx*Sy))/delta
c = ((Sxx*Sy)-(Sx*Sxy))/delta;
%---------------------------------------------
yd = zeros(1,Nu+1);
yd(2:Nu+1)=d(1:Nu);
y = m.*yd + c;
%---------------------------------------------
%Error on gradient
sigma = sqrt(S/delta)
%Chi sq
Chisq = sum(((p-y(2:Nu+1))./(errgrad)).^2)
ChisqNDF = Chisq/7
%---------------------------------------
%Graphs
errorbar(d,p,errgrad,'bx')
axis([0 18 0 900])
xlabel('1/sqrt(dQ/dT)')
ylabel('\DeltaSqrt (2J_{z,max})/\Delta\sigma [m^{-1/2}]')
hold on
plot(yd,y)
%--------------------------------------------
```

<u>Function for Calculating the Maximum Amplitude Given a Rate of Acceleration and Standard Deviation of Alignment Errors:</u>

```
function ex5Nturns(turnset, N)
global Q qe LightSpeed Amax GradTune
CT = 42*N;   %number of cells traversed
L = 16.57;   % (m) Circumference
%Quadrupole details ( Column 1 is focussing and 2 is defocussing,
%row 1 is field gradient and 2 is lattice length)
lqf = 58.782e-3; %length of horizontally focusing quad
lqd = 75.699e-3; %length of horizontally defocusing quad
Q = [6.7, -4.9
     lqf, lqd];

qe = 1.602e-19; %electron charge
LightSpeed = 2.998e8;   %  (m/s)  speed of light
%Assumes straight paths!
T0 = L/LightSpeed; %time taken for one revolution
TDF = 0.274571/LightSpeed; %time taken to travel from defocussing to
focussing quad
TFD = 0.120023/LightSpeed; %time taken to travel from focussing to
defocussing quad
%-------------------------------------------------
% set matrices of before (1) and after (2) position and velocity
x1 = zeros(1, CT);  %
v1 = zeros(1, CT);  % x1(m)displacement & v1(m/s) velocity after one cell
A1 = zeros(1, CT);
beta1 = zeros(1, CT);
tunegraph = zeros(1,CT);
%-------------------------------------------------
%Acceleration parameters
%Energy range
Estart = 10.75; %Injection energy MeV
Estop = 20.75; %Extraction energy MeV
deltaE = (Estop - Estart)/CT; %energy increase per cell

for nxsigmamin = 1:500
%-------------------------------------------------
%distribution of misalignments and associated forces
mu=0; %mean
sigma= nxsigmamin*(1E-6)/5; %standard deviation
seed = nxsigmamin^2; %to provide repeatable values for testing
F = gauerr(mu, sigma, seed);

%--------------------------------------------------
% Particle Start parameters
tunemax = (0.0549*Estart^2) - (2.4572*Estart) + 32.4479;
tunemin = (0.0549*Estop^2) - (2.4572*Estop) + 32.4479;
freq = tunemax / T0;
wb = 2*pi*freq;
GradTune(1,turnset) = (tunemax - tunemin)/N; %change in tune per turn,
linear approximation.
beta1(1) = L/(2*pi*tunemax); % beta start value
x1(1) = 0;   % (m) start displacement
v1(1) = 0;    % (m/s) start velocity
A1(1) = sqrt(x1(1)^2 + v1(1)^2 / wb^2);
%counting
c=1;
for c1 = 1:(CT-1),
  energy = Estart + c1*deltaE;
```

```
  tune = (0.0549*energy^2) - (2.4572*energy) + 32.4479;
  tunegraph (c1) = tune;
  freq = tune / T0;
  wb = 2*pi*freq;

  dvF = (F(c,3) * LightSpeed * Q(2,1))/(energy*1e6*qe); %transverse
velocity kick at focussing quad
  dvD = (F(c,4) * LightSpeed * Q(2,2))/(energy*1e6*qe); %transverse
velocity kick at defocussing quad

  vector1 = [x1(c1)
            v1(c1)];

  M = M1(wb, TDF);
  vector2 = M * vector1;   %travel from previous defocussing quad to
following focussing quad
  vector2(2)=vector2(2) + dvF; %adds kick from horizontally focussing quad
to vector
  M = M1(wb, TFD);
  vector2 = M * vector2;  %travel from previous focussing quad to following
defocussing quad
  vector2(2)=vector2(2) + dvD; %adds kick from horizontally defocussing
quad to vector

  x1(c1+1) = vector2(1);
  v1(c1+1) = vector2(2);

  A1(c1+1) = sqrt(x1(c1+1)^2 + (v1(c1+1)^2 / wb^2));
  beta1(c1+1) = L/(2*pi*tune);
  c = c+1;
  if c>42
      c=1;
  end
end
% Maximum amplitude for nxsigmamin errors over N turns
A1 = A1 ./sqrt(beta1);
Amax(nxsigmamin, turnset) = max(A1);
end
end
```

<u>Random Cell Alignment Generator (gauerr.m):</u>

Refer to gauerr.m in the first programming section.

<u>SHM Transfer Matrix (M1.m):</u>

Refer to M1.m in first programming section.

4. Matlab program (ex6maxamp4startamp.m) for calculating the physical aperture:

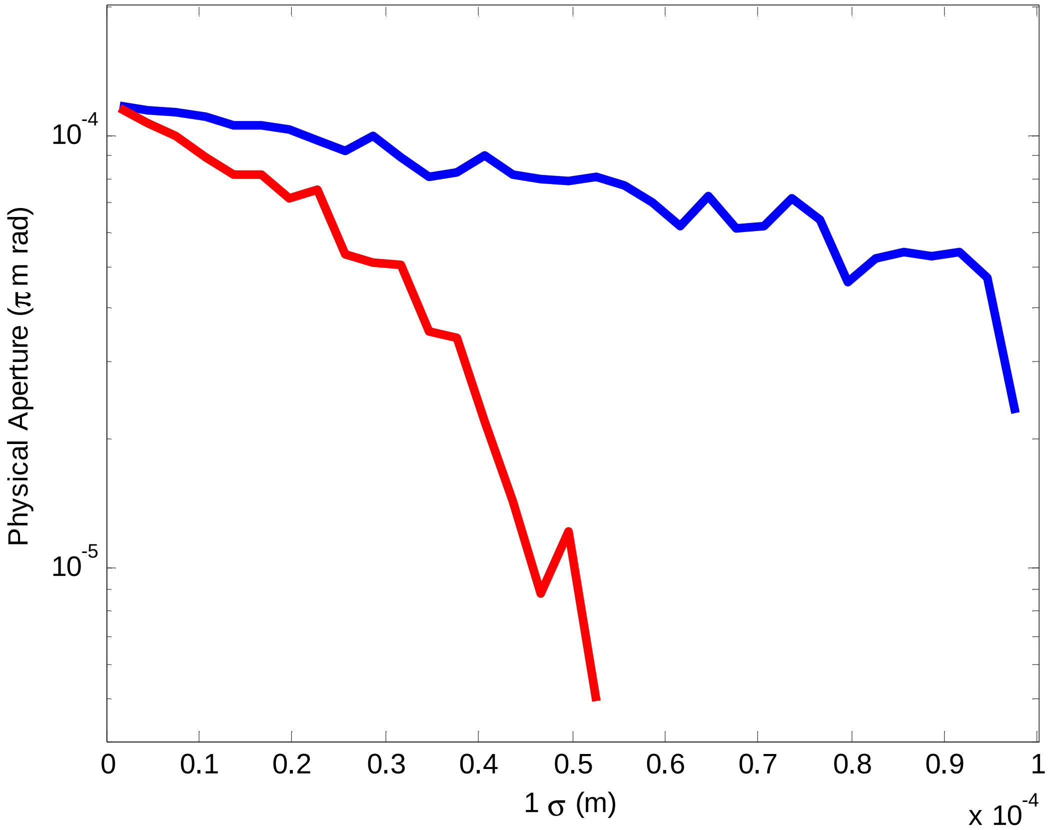

Main Program

```
clear all

% to simulate the effect of 84 kicks per revolution
% on an electron in EMMA assuming uniform focusing strength
% with the aim of estimating the physical aperture for 100 turns
% and 1000 turns.
%-------------------------------------------------

N0 = [100, 1000];    % no. of turns
n=numel(N0);  %number of elements in the array N0
global DA
DA = zeros(500,n);
DAplot = zeros(33,n);
sigmaA=zeros(33);
for turnset = 1:n
    N = N0(turnset);
    ex6routine(turnset, N);
end

%-----------------------------------------
sigma = [1:500]' .*((1e-6)/5);
    for b=1:n
  %----------------------
    Amid = -7;
    for A = 1:33
        Amid = Amid+15;
```

```
        sigmaA(A) = sigma(Amid);
        avg = 0;
        for range = -7:7
            f=Amid+range;
            avg = avg + DA(f,b);
        end
        avg = avg/15;
        DAplot(A,b) = avg;
    end

    %----------------------
  if b==1
    %scatter(sigma, DA(1:500,b), 20,'bx')
    sig1 = sigmaA(1:33);
    Da1 = DAplot(1:33,1);
    semilogy(sig1,Da1,'blue','LineWidth',3)
    xlabel('1 \sigma (m)')
    ylabel('Dynamic Aperture (\pi m rad)')
    axis([0 1e-4 10e-7 1e-4])
    hold on
  end
  if b==2
    %scatter(sigma, DA(1:500,b), 20,'rx')
    sig = sigmaA(1:17);
    Da = DAplot(1:17,2);
    semilogy(sig,Da,'red','LineWidth',3)
  end
  end
  hold off
```

Function for Calculating the Maximum Start Amplitude of a Particle which is Accelerated to the Extraction Energy Without Incidence Upon Accelerator Wall Given A Particular Standard Deviation of Error Distribution and Rate of Acceleration

```
function ex6routine(turnset, N)
global Q qe LightSpeed DA
%--------------------------------------------------
%Accelerator Constants
CT = 42*N;   %number of cells traversed
L = 16.57;   %(m) Circumference

%Quadrupole details ( Column 1 is focussing and 2 is defocussing,
%row 1 is field gradient and 2 is lattice length)
lqf = 58.782e-3; %length of horizontally focusing quad
lqd = 75.699e-3; %length of horizontally defocusing quad
Q = [6.7, -4.9
     lqf, lqd]; %Quadrupole gradients and lengths

qe = 1.602e-19; %electron charge
LightSpeed = 2.998e8;   %  (m/s)  speed of light
%Assumes straight paths!
T0 = L/LightSpeed; %time taken for one revolution
TDF = 0.274571/LightSpeed; %time taken to travel from defocussing to
focussing quad
TFD = 0.120023/LightSpeed; %time taken to travel from focussing to
defocussing quad
```

```
%-----------------------------------------------
% set matrices of position and velocity
x1 = zeros(1, CT);  %
v1 = zeros(1, CT);  % x1(m)displacement & v1(m/s) velocity after one cell

%-----------------------------------------------------
%Acceleration parameters
%Energy range
Estart = 10.75; %Injection energy MeV
Estop = 20.75; %Extraction energy MeV
deltaE = (Estop - Estart)/CT; %energy increase per cell
SA=[0:0.1:11].*1e-3; %Start amplitudes
tunestart = (0.0549*(Estart^2))-(2.4572*Estart)+32.4479;
beta = L/(2*pi*tunestart);
root2J=8.9e-3/sqrt(beta);
%-----------------------------------------------------
%distribution of misalignments and associated forces
mu=0; %mean
for nxsigmamin = 1:500
nxsigmamin
sigma= nxsigmamin*(1E-6)/5; %standard deviation
seed=nxsigmamin^2;
F = gauerr(mu, sigma, seed);
k=0;
startamp = 0;
while k == 0
    startamp = startamp +1; %increases start amplitude from zero to half
aperture
    %-------------------------------------------------
    % Particle Start parameters
    x1(1) = SA(startamp);   % (m) start displacement
    v1(1) = 0;    % (m/s) start velocity
    %counting
    c=1; %individual cell number (1-42)
    %-------------------------------------------------
    %Calculate maximum amplitude for trial start conditions
        A1 = 0;
        JA1=0;
        c1 = 0;
        while JA1<root2J && c1<=(CT-1) %while amplitude is less than
aperture size and acceleration is not complete
        c1=c1+1; %counts total number of cells
        energy = Estart + c1*deltaE;
        tune = (0.0549*(energy^2))-(2.4572*energy)+32.4479;
        freq = tune / T0;
        wb = 2*pi*freq;

        dvF = (F(c,3) * LightSpeed * Q(2,1))/(energy*1e6*qe); %transverse
velocity kick at focussing quad
        dvD = (F(c,4) * LightSpeed * Q(2,2))/(energy*1e6*qe); %transverse
velocity kick at defocussing quad

        vector1 = [x1(c1)
                   v1(c1)];

        M = M1(wb, TDF);
        vector2 = M * vector1;   %travel from previous defocussing quad to
following focussing quad
        vector2(2)=vector2(2) + dvF; %adds kick from horizontally focussing
quad to vector
```

```
        M = M1(wb, TFD);
        vector2 = M * vector2;  %travel from previous focussing quad to
following defocussing quad
        vector2(2)=vector2(2) + dvD; %adds kick from horizontally
defocussing quad to vector

        x1(c1+1) = vector2(1);
        v1(c1+1) = vector2(2);
        A1 = sqrt(x1(c1+1)^2 + (v1(c1+1)^2 / wb^2));
        beta1 = L/(2*pi*tune);
        JA1 = A1/sqrt(beta1);
        c = c+1;
            if c>42
              c=1;
            end
        end

    %---------------------------------------------------

    DA (nxsigmamin, turnset) = ((SA(startamp)^2))/(pi*(beta));
            if JA1 > root2J
                k=1;
            end

end
end
end
```

<u>Random Cell Alignment Generator (gauerr.m):</u>

Refer to gauerr.m in the first programming section.

<u>SHM Transfer Matrix (M1.m):</u>

Refer to M1.m in first programming section.

Bibliography

Websites:

BASROC. (2006) *British Accelerator Science and Radiation Oncology Consortium.* Available at http://www.basroc.org.uk/index.htm (Last accessed: 10 May 2010).

Conform (2007) *EMMA cell layout.* Available at http://www.astec.ac.uk/emmafiles/magnets/EMMAcelllayout.ppt (Last accessed: 10 May 2010).

Conform (2007) *EMMA geometry*. Available at http://www.astec.ac.uk/emmafiles/magnets/EMMA Geometry.xls (Last accessed: 10 May 2010).

Conform (2007) *EMMA layout phase 2.* Available at http://www.conform.ac.uk/documents/emma/dwg-drawings/207-10324-C-EMMA-LAYOUT-PHASE-2-colour.jpg (Last accessed: 10 May 2010).

Conform (2007) *EMMA magnet cross section*. Available at http://www.astec.ac.uk/emmafiles/magnets/Emma%20Magnet%20Cross%20Section%2028-9-06.doc (Last accessed: 10 May 2010)

Conform. (2006) *FFAG magnets*. Available at: http://www.conform.ac.uk/documents/emma/mag-magnets/ffag%20magnets.pdf (Last accessed: 10 May 2010).

Paul, H. (2009) *Depth Dose Curves*. Available at http://en.wikipedia.org/wiki/File:Depth_Dose_Curves.jpg (Last accessed: 10 May 2010).

Tarr, M. (2007) *Dielectric Properties*. Available at http://www.ami.ac.uk/courses/topics/0184_dp/index.html (Last accessed: 10 May 2010).

Books:

Lee, S.Y. (2004) *Accelerator physics.* 2nd edn. London : World Scientific.

Lemoigne, Y. (2009) *Radiotherapy and Brachytherapy* [electronic book]. 1st edn. Dordrecht: Springer Netherlands.

Mayles, P., Nahum, A., & Rosenwald J.C. (2007) *Handbook of radiotherapy physics: theory and practice.* 1st edn. London: Taylor & Francis.

Wille, K. (2000) *The physics of particle accelerators : an introduction.* 1st edn. Oxford: Oxford University Press.

Wilson, E. (2001) *An introduction to particle accelerators*. 1st edn. New York: Oxford University Press.

Wu Chao, A. & Tigner, M. (1999) *Handbook of accelerator physics and engineering.* 1st edn. London: World Scientific.

Edwards,D. & Syphers,M.(1993) *An Introduction to the Physics of High Energy Accelerators.* 1st edn. Weinheim: Wiley-VCH.

Journals:

Bonnett, D.E., Kacperek, A., Sheen M.A., Goodall, R. & Saxton T.E. (1993) *The 62 MeV proton beam for the treatment of ocular melanoma at Clatterbrigde*. British Journal of Radiology. Volume 66, p.907-914.

Machida, S. (2008) *Resonance Crossing and Dynamic Aperture in Non-scaling Fixed Field Alternating Gradient Accelerators*. The American Physical Society. Volume 11, 094003.

Miscellaneous:

Berg, J. (2007) *The EMMA Experiment.* ICFA Beam Dynamics Newsletter, Issue 43, p.60-74

Brandt, D. (2004) *Accelerator basics.* Accelerator basics notes. Available from: http://cas.web.cern.ch/CAS/Warrington/PDF/Brandt5.pdf

Edgecock, R. (2009) *FFAGs for Radiotherapy*. IOP Mayneord Phillips Summer Schools notes. Available at http://mpss.iop.org/Summer_School/2009/Programme2009/EdgecockFFAGs.pdf

Fenwick, J. (2010) *Biological Modelling.* PHYS384:Radiation Therapy Applications notes.

Mosthaf, J.M., Peters, A., Hanke, S., Scheloske, S., Vollmer, S. & Fleck, T. (2008) *Overview of the communication structure of the hit accelerator control system.* Conference proceedings of PCaPAC08. Available from: http://accelconf.web.cern.ch/Accelconf/pc08/papers/wep002.pdf

Press, W.H. et al. (1995) *Numerical recipes in C [computer disk]* Cambridge University Press. 2nd edn. V2.06.

Wolski, A. (2006) *Effects of Linear Imperfections.* Linear Dynamics lecture notes. Available at http://pcwww.liv.ac.uk/~awolski/Teaching/LinearDynamics/LinearDynamics-Lecture10.pdf